AD-A134 428 STATISTICAL ASPECTS OF ICE GOUGING ON THE ALASKAN SHELF 1/
OF THE BEAUFORT SEA(U) COLD REGIONS RESEARCH AND
ENGINEERING LAB HANOVER NH W F WEEKS ET AL. SEP 83
UNCLASSIFIED CRREL-83-21 F/G 8/10 NL

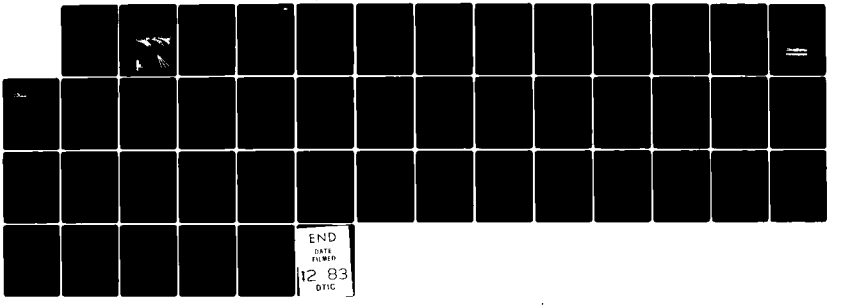

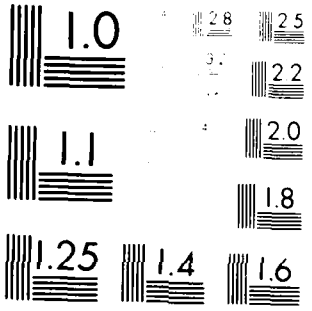
1.0
2.8
2.5
2.2
1.1
2.0
1.8
1.25
1.4
1.6

(12)

REPORT 83-21

US Army Corps
of Engineers
Cold Regions Research &
Engineering Laboratory

Statistical aspects of ice gouging on the Alaskan Shelf of the Beaufort Sea

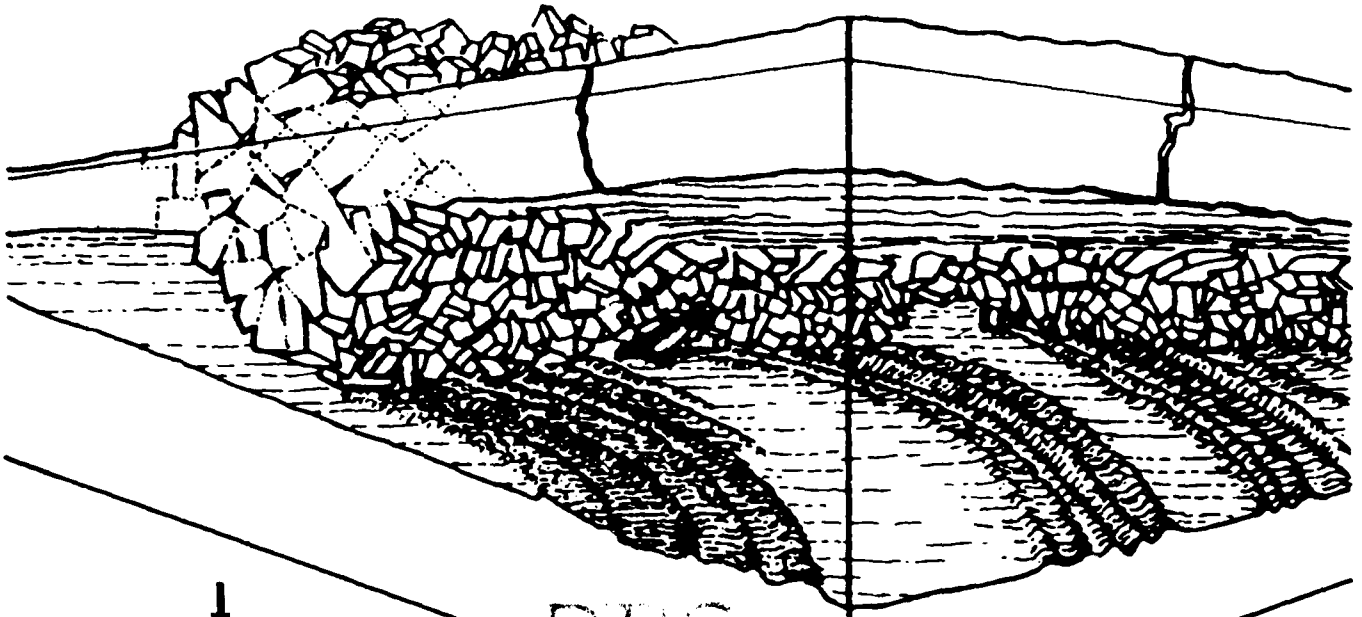

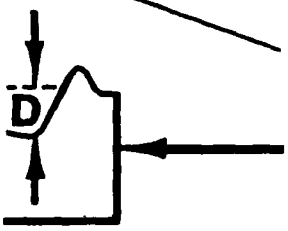

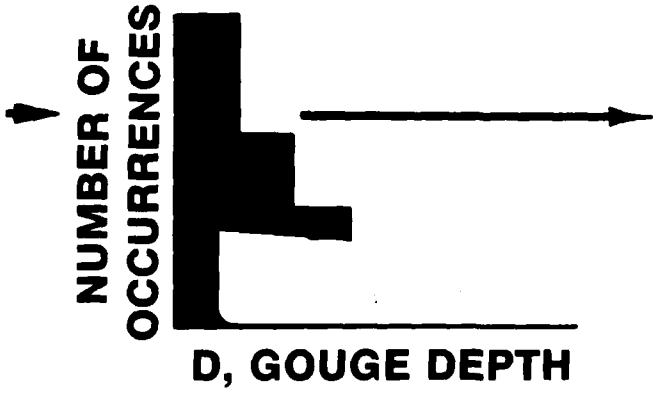

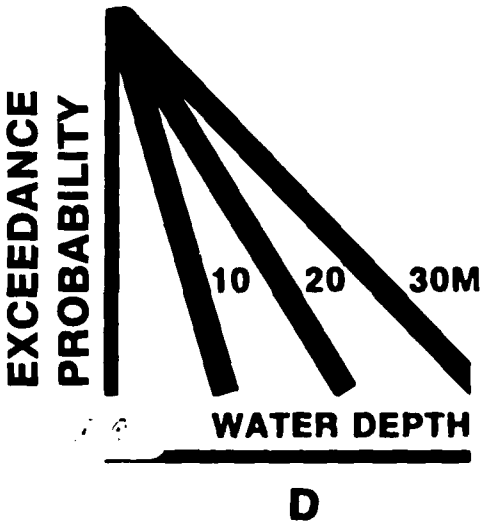

For conversion of SI metric units to U.S./ British customary units of measurement consult ASTM Standard E380, Metric Practice Guide, *published by the American Society for Testing and Materials, 1916 Race St., Philadelphia, Pa. 19103.*

CRREL Report 83-21

September 1983

Statistical aspects of ice gouging on the Alaskan Shelf of the Beaufort Sea

W.F. Weeks, P.W. Barnes, D.M. Rearic and E. Reimnitz

Prepared for
NOAA/DEPARTMENT OF COMMERCE
Approved for public release; distribution unlimited

Unclassified

SECURITY CLASSIFICATION OF THIS PAGE (When Data Entered)

REPORT DOCUMENTATION PAGE

READ INSTRUCTIONS BEFORE COMPLETING FORM

1. REPORT NUMBER: CRREL Report 83-21	2. GOVT ACCESSION NO.: A134428
3. RECIPIENT'S CATALOG NUMBER:	
4. TITLE (and Subtitle): STATISTICAL ASPECTS OF ICE GOUGING ON THE ALASKAN SHELF OF THE BEAUFORT SEA	5. TYPE OF REPORT & PERIOD COVERED:
	6. PERFORMING ORG. REPORT NUMBER:
7. AUTHOR(s): W.F. Weeks, P.W. Barnes, D.M. Rearic and E. Reimnitz	8. CONTRACT OR GRANT NUMBER(s):
9. PERFORMING ORGANIZATION NAME AND ADDRESS: U.S. Army Cold Regions Research and Engineering Laboratory, Hanover, New Hampshire 03755	10. PROGRAM ELEMENT, PROJECT, TASK AREA & WORK UNIT NUMBERS:
11. CONTROLLING OFFICE NAME AND ADDRESS: Outer Continental Shelf Environmental Assessment Program, Office of Marine Pollution Assessment, NOAA/Department of Commerce, Juneau, Alaska 99802	12. REPORT DATE: September 1983
	13. NUMBER OF PAGES: 40
14. MONITORING AGENCY NAME & ADDRESS (if different from Controlling Office):	15. SECURITY CLASS. (of this report): Unclassified
	15a. DECLASSIFICATION/DOWNGRADING SCHEDULE:

16. DISTRIBUTION STATEMENT (of this Report)

Approved for public release; distribution unlimited.

17. DISTRIBUTION STATEMENT (of the abstract entered in Block 20, if different from Report)

18. SUPPLEMENTARY NOTES

19. KEY WORDS (Continue on reverse side if necessary and identify by block number)

Arctic Ocean
Arctic regions
Beaufort Sea
Ice
Ice gouging
Sea ice
Offshore drilling
Offshore structures

20. ABSTRACT (Continue on reverse side if necessary and identify by block number)

The statistical characteristics of ice-produced gouges in the sea floor along a 190-km stretch of the Alaskan coast of the Beaufort Sea between Smith Bay and Camden Bay are studied, based on 1500 km of precision fathometry and side-looking sonar records that were obtained between 1972 and 1979 in water depths to 38 m. The probability density function of the gouge depths into the sediment is represented by a simple negative exponential over four decades of gouge frequency. The exceedance probability function is, therefore, $e^{-\lambda d}$, where d is the gouge depth in meters and λ is a constant. The value of λ shows a general decrease with increasing water depth, from 9 m^{-1} in shallow water to less than 3 m^{-1} in water 30 to 35 m deep. The deepest gouge observed was 3.6 m, from a sample of 20,354 gouges that have depths greater than or equal to 0.2 m. The dominant gouge orientations are usually unimodal and reasonably

DD FORM 1 JAN 73 1473 EDITION OF 1 NOV 65 IS OBSOLETE

Unclassified

SECURITY CLASSIFICATION OF THIS PAGE (When Data Entered)

20. Abstract (cont'd).

clustered, with the most frequent alignments roughly parallel to the general trend of the coastline. The value of $\bar{N}_1$, the mean number of gouges (deeper than 0.2 m) per kilometer measured normal to the trend of the gouges, varies from 0.2 for protected lagoons to 80 in water between 20 and 38 m deep in unprotected offshore regions. The distribution of the spacings between gouges as measured along a sampling track is a negative exponential. The form of the frequency distribution of N_1 varies with water depth and is exponential for lagoons and shallow offshore areas, positively skewed for 10 to 20 m depths off the barrier islands, and near-normal for deeper water. As a Poisson distribution gives a reasonable fit to the N_1 distributions for all water depths, it is suggested that gouging can be taken as approximating a Poisson process in both space and time. The distributions of the largest values per kilometer of gouge depths, gouge widths, and the heights of the lateral embankments of sediments plowed from the gouges are also investigated. Limited data on gouging rates give an average of 5 gouges per kilometer per year. Examples are given of the application of the data set to hypothetical design problems associated with the production of oil from areas in the Alaskan portion of the Beaufort Sea.

PREFACE

This report was prepared by Dr. W.F. Weeks, *Glaciologist*, U.S. Army Cold Regions Research and Engineering Laboratory, Hanover, New Hampshire, and Dr. P.W. Barnes, L.M. Rearic, and Dr. E. Reimnitz, Geologists, of the Pacific Arctic Branch of Marine Geology, U.S. Geological Survey, Menlo Park, California. The cover illustration was also a cooperative effort of the USGS and CRREL, with the line drawing of ice gouging contributed by Tau Rho Alpha of the Survey and the remainder of the graphics designed by Tom Vaughan of CRREL.

Funding for this study was provided by the Minerals Management Service through an interagency agreement with the National Oceanic and Atmospheric Administration as part of the Outer Continental Shelf Environmental Assessment Program (OCSEAP), which responds to the needs of petroleum development of the Alaskan continental shelf.

The authors would like to thank Gunter Weller, Dave Norton, and Bill Sackinger for allowing the continuing data collection effort that made this study possible. One of the authors (Weeks) would also like to thank the Office of Naval Research for support during the year he spent at the Naval Postgraduate School in the ONR Chair of Arctic Marine Science as well as Don Gaver and Pat Jacobs of the NPS Operations Research Department for their council and encouragement. We have also profitted from the reviews and advice of Ed Phifer, John Kreider, Richard Larrabee, and P.W. Marshall of Shell, of Hans Jahns and Albert Wang of EXXON, of Paul Teleki of the U.S. Geological Survey and of Austin Kovacs, Malcolm Mellor, and Darryl Calkins of CRREL. Whatever the shortcomings of this paper, they clearly are not the result of a lack of good advice.

CONTENTS

ILLUSTRATIONS

TABLES

STATISTICAL ASPECTS OF ICE GOUGING ON THE ALASKAN SHELF OF THE BEAUFORT SEA

W.F. Weeks, P.W. Barnes, D.M. Rearic and E. Reimnitz

INTRODUCTION

A survey of the bathymetry of the Beaufort Sea shows that large areas of this marginal sea of the Arctic Ocean have water depths of less than 60 meters. In this region ungrounded pressure ridge keels may protrude downward for at least 50 m, and ice floes containing such keels drift in a general pattern from east to west along the Beaufort coast. Therefore it is reasonable to presume that such sea ice masses could interact with the sea floor. Indeed, ice-related disturbances of the sea floor have been inferred for some decades from observations of sea floor sediments entrained in obviously grounded ice masses (Kindle 1924). At the time, such processes were largely of academic interest, and there was little motivation to explore them systematically.

With the discovery of oil and gas along the margins of the Beaufort Sea at Prudhoe Bay and off the Mackenzie Delta, processes modifying the floor of the Beaufort Sea became of interest due to their possible effect on offshore design and operations. Early side-scan sonar and precision fathometry data coupled with diving observations (Shearer et al. 1971, Kovacs 1972, Pelletier and Shearer 1972) showed clearly that much of the sea floor was heavily marked by long linear depressions, which we will refer to as gouges, produced by the ploughing action of ice. The depths and widths of gouge incisions in the sea floor reached several meters and several tens of meters respectively, with gouges occurring as both individual isolated events and as multiple events, presumably produced by projections on the same pressure ridge keel gouging the sea floor as part of the same ice motion (Kovacs and Mellor 1974, Reimnitz and Barnes 1974).

In this paper we discuss some random-appearing aspects of ice-produced gouges that occur along a 190-km stretch of the coast of the Beaufort Sea between Smith Bay and Camden Bay (refer to Fig. 1). We also include a brief discussion of the statistical concepts and techniques that are utilized. As much of the study area is part of the 1979, 1982, and 1984 lease sales offered by the State of Alaska and the Federal Government, we believe that the results reported here are of immediate interest to the engineering community involved in offshore design for the Beaufort Sea as well as of long-term interest to the scientific community interested in near-shore processes in shallow, ice-covered seas. The paper concludes by discussing some of these potential applications.

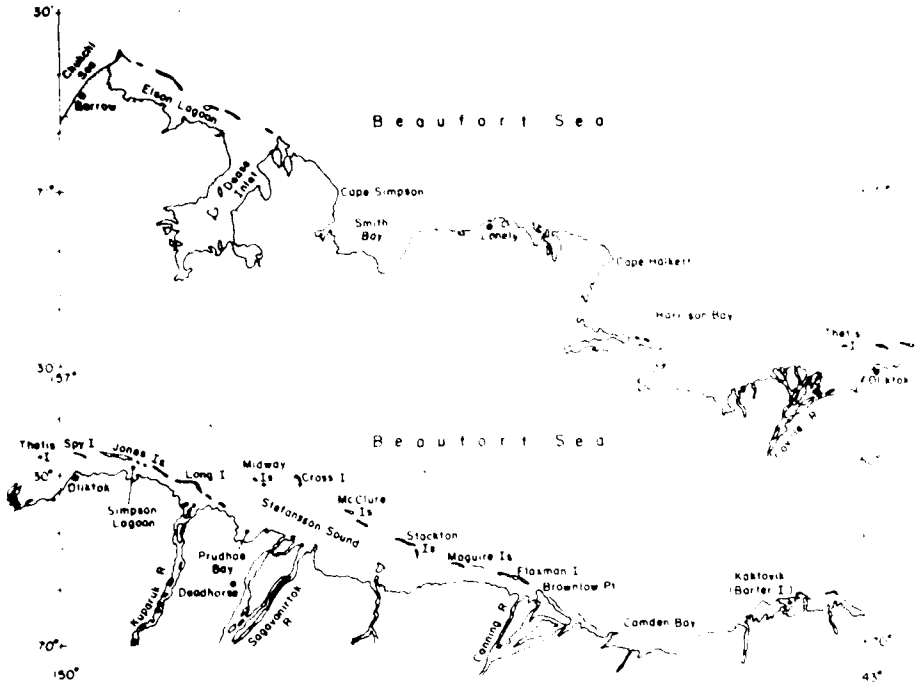

Figure 1. Part of the Alaskan coastline of the Beaufort Sea.

BACKGROUND AND ENVIRONMENTAL SETTING

Because of their importance to offshore design in arctic areas, ice-produced gouges have been the subject of a number of investigations, especially since they were recognized as a recurring sea-floor feature in the shallow portions of ice-covered seas. Rather than review this literature here, we will simply mention publications of general interest that provide more exhaustive reference lists. Reviews of early work can be found in Kovacs (1972) and Kovacs and Mellor (1974). Early studies off the Mackenzie Delta are described by Shearer et al. (1971), Pelletier and Shearer (1972), and by Kovacs and Mellor (1974). Early work off the Alaskan coast is reported by Skinner (1971), Reimnitz et al. (1972, 1973), Barnes and Reimnitz (1974), and Reimnitz and Barnes (1974). More recent work is discussed by Shearer and Blasco (1975), Hnatiuk and Brown (1977), Reimnitz et al. (1977a,b; 1978), Barnes et al. (1978), and Barnes and Reimnitz (1979). These studies provide a description of the nature of the gouges, the characteristics of the ice involved in the gouging process, the general distribution of gouging along the coast, and, to some extent, the forces involved in the process and the rates of gouge recurrence. In most of the studies little attention was paid to how the observed gouge parameters varied or to methods for estimating infrequent gouging events, such as the formation of deeper gouges. Exceptions to this are the papers by Lewis (1977a,b) and Wahlgren (1979a,b), which examine the statistical aspects of the gouges located in the general area of the Mackenzie Delta.

Present evidence suggests that the Beaufort Sea shelf has been relatively stable during the last 10,000 years (i.e. major tectonic or glacio-isostatic adjustments have not taken place [Hopkins 1967]). As sea level has risen approximately 35 m in this time period, the entire sea floor of the present study area was land in the geologically recent past. The gentle slope of the present land surface continues northward to a water depth of 60 to 70 m, where the shelf break occurs (Barnes and Reimnitz 1974). Figure 2 gives generalized bathymetry for the study area. The broad, gently sloping shelf is quite evident. When the sea-floor topography in the study area is examined in more detail it is found to be very complex (see map given as Appendix A; Barnes and McDowell 1978). The most notable features are a number of submerged

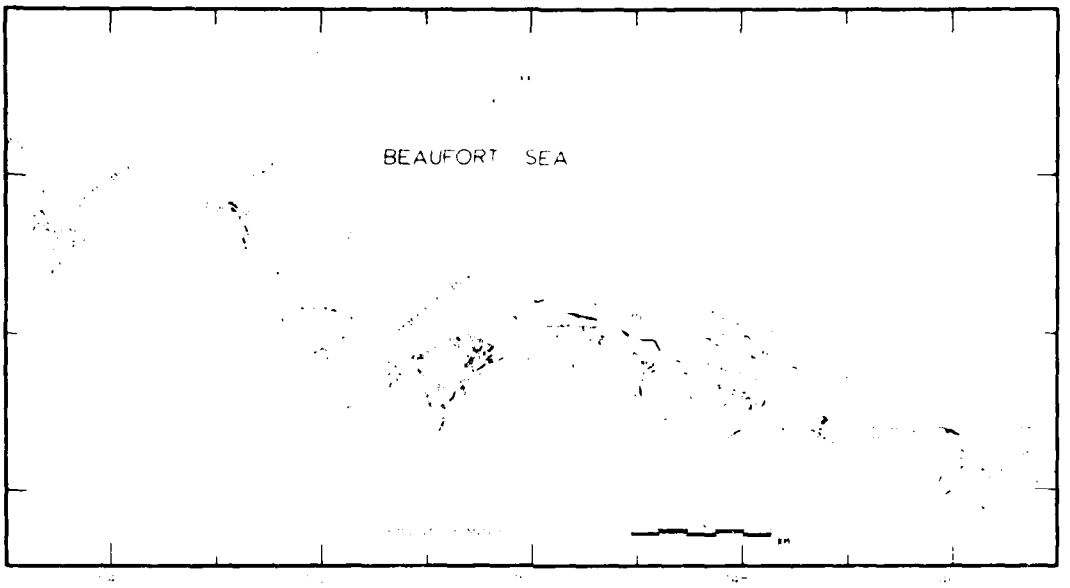

Figure 2. Generalized bathymetric chart of the study area.

shoals and bottom irregularities that have been related to ice zonation (Reimnitz et al. 1977b). On the scale of the gouging it is even more complex (not shown). Holocene sediments (chiefly poorly sorted silty clays and sandy muds) exhibit maximum thicknesses of 5 to 10 m over the inner shelf. The seabed of the region is characterized by extreme diversity and variability of sediment types, seabed character, and sedimentary structures. Sedimentary structures are dominated by wave- and current-related processes inshore of 10 m, by ice-, wave-, and current-related processes between 10 and 20 m, and by primarily ice-related processes out to water depths of 50 m or more, where water-related depositional processes again dominate. Noteworthy is the nearly ubiquitous occurrence of stiff silty clays in outcrops on the inner shelf.

The oceanographic regime of the region has been little studied. The near-shore circulation appears to be strongly wind-driven during the summer, with flushing rates and currents closely related to local winds. The most striking oceanographic events are waves, currents, and surges resulting from late summer storms. Local sea-level rises of 3 m coupled with 3-m waves have been observed. Limited data during the summer suggest a general westward water motion produced by the prevailing easterlies, but wind-driven reversals are not rare. During the winter the dominant currents on the inner shelf are believed to be the results of thermohaline drainage out of the r ıore regime of dense, cold, salt-rich water pr ·y the formation of sea ice (Mathews 1981,

The ice regime of the region shows great changes with season and distance from shore. During the summer, ice conditions are extremely variable. Much of the study area is commonly ice-free, with the southern edge of the multiyear pack ice occurring between 10 and 100 km offshore. New ice starts to form in October; during the early stages of its formation ice movement velocities nearshore are similar to velocities offshore (5 km day on the average with highs of 35 km day during storms [Thomas and Pritchard 1979]). As the new ice thickens, velocities decrease at nearshore locations until the ice becomes truly fast, experiencing typical motions of only a few tens of meters over the remainder of the winter (on occasion motions exceeding 1000 m have been observed [Kovacs 1979]). At offshore locations, motions also decrease somewhat but average movements still remain significant (1 to 2 km day^{-1}). At times the whole ice pack may be nearly motionless for several days. Numerous pressure ridges form in the moving ice, and in shallower areas many of these ridges become grounded. Areas of particularly heavy groundings occur off the barrier islands in water depths of roughly 15 to 20 m. In areas such as Harrison Bay that are not protected by barrier islands, large grounded ridges occur in shallower waters (roughly 10-m depth). Once the grounded

ridge or stamukhi zone develops, the ice shoreward of this feature remains relatively motionless until spring.

During spring, which on the coast of the Beaufort Sea occurs in June, melting allows formerly bottom-fast ice near the shore to float. This allows the nearshore ice to become mobile once again. Many examples of ice pile-up and over-ride on beaches are known to have occurred during this period (Kovacs and Sodhi 1980). Within the constraints presented by the coast and by grounded ridges and rubble fields, the nearshore ice remains mobile throughout the summer unless it disappears by melting or is blown out to sea. However, the massive areas of grounded ridges and rubble often remain grounded throughout most or even all of the summer (Kovacs 1976, Barnes and Reimnitz 1979). Associated with these grounded ice features at the 18- to 20-m water depth is a break in the seabed slope and changes in gouge character and sediment texture (Reimnitz and Barnes 1974). Additional information on the oceanography and sedimentology of the study area can be found in APO (1978).

DATA COLLECTION AND TERMINOLOGY

Seven years of data obtained between 1972 and 1979 (excluding 1974) were used in the present study, with a total sample trackline length of approximately 1500 km. Data were collected from the research vessels *Loon* and *Karluk* using a side-scan sonar and a precision fathometer (200 kHz). Both systems were capable of resolving bottom relief of less than 10 cm. The side-scan records covered the sea floor beneath the ship in 200-m or 250-m swaths, depending on scale selection. Figures 3 and 4 are a representative sonograph and a fathogram respectively. The tracks were spaced to provide fairly evenly distributed sampling along the coast between Smith Bay and Camden Bay. Data were obtained both inside and seaward of the barrier islands to the 38-m isobath. Figure 5 shows the locations of the different sampling lines. The trackline navigation was plotted in 1-km segments. The sonographs and fathograms were also divided into 1-km segments and correlated directly with the navigation. As some aspects of the data interpretation are subjective, all the counting and measuring was performed by one individual (D. Rearic) to minimize variations.

A complete ice gouge data record sheet showing all measurements is given by Rearic et al. (1981). A description of the general techniques that were used in analyzing the sonographs and fathograms is given in Barnes et al. (1978), but a few important points affecting the parameters used in the present study should be mentioned:

Average water depth ($\bar{z}$). This was determined by averaging the water depths observed at the start

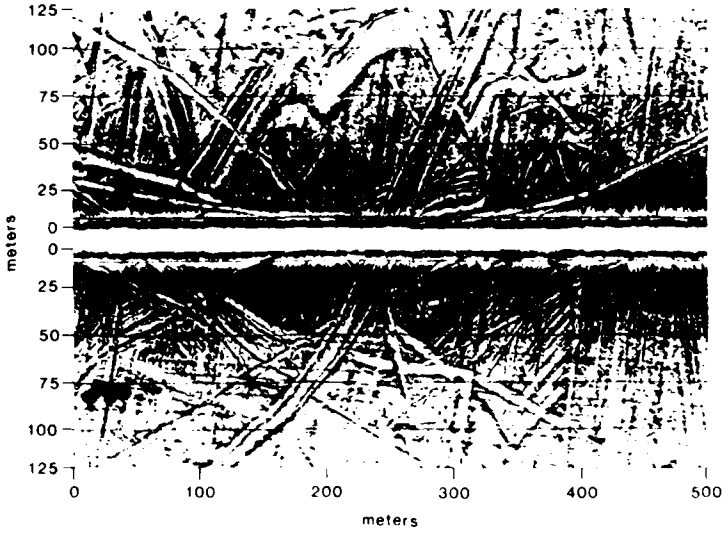

Figure 3. Sonograph of ice-gouged sea floor. Water depth is 20 m. Record taken 20 km NE of Cape Halkett.

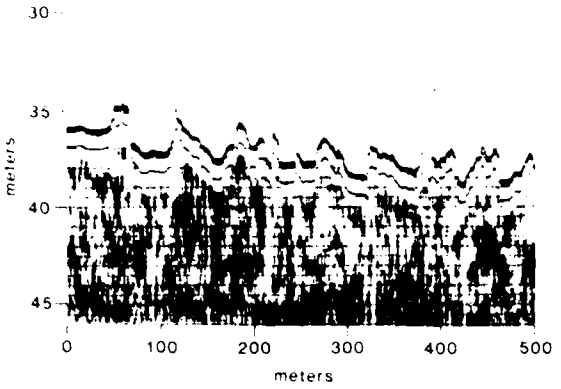

Figure 4. Fathogram of ice-gouged sea floor. Water depth is 36 m. Record taken 25 km NE of Cape Halkett.

and at the end of each 1-km section; as z changes are usually gradual and reasonably smooth, z should be a reasonable approximation to a spatially integrated value.

Dominant gouge orientation (θ). Templates were used to remove horizontal exaggeration from the sonographs and to obtain all measurements of the estimated dominant orientation to within 5° true. It should be noted that the gouge orientations within each line segment are variable (see Fig. 3).

Spatial gouge frequency (N). In determining the number of gouges per kilometer of sampled track (N), every feature on the fathograph presumed to result from ice contact with the bottom was counted, including individual gouges produced by different segments of what was probably the same pressure ridge keel (our interest is in the number of gouges in the bottom, not in the number of ice events); these N values were then corrected in order to estimate $N_\perp$, the expected number of gouges that would have been seen on a 1-km sampling line if the ship's track were oriented normal to the dominant gouge trend. This correction was made by using $N_\perp = N \sin\alpha$, where α is an acute angle between the ship's track and the gouge orientation. As most gouges are oriented parallel to the coast and the majority of the sampling lines were roughly normal to the coast, these corrections were usually small. Gouges with depths of less than 0.2 m were not counted, as it was often difficult to identify positively all of these small gouges on the fathogram. Actually, in the original data tabulations (Rearic et al. 1981) a value was given for the number of gouges in the 0 to 0.2-m range that could be distinguished on the sonar record. Although this value can be useful, it should not be combined with the data on gouges deeper than 0.2 m, as it includes a number of gouges that do not cross beneath the ship's track (i.e. that would not appear on the fathometer track).

Gouge depth (d). The depth was measured (on the fathometer track) vertically from the level of the (presumably undisturbed) adjacent sea floor to the lowest point in the gouge (see Fig. 6). Values were grouped in 20-cm class intervals; in some cases, because of factors such as ground swell and wind chop, it was only possible to determine the number of gouges that have depths greater than a specified value, so gouges less than 0.2 m deep were not considered. Each individual gouge was measured. The maximum gouge depth (d_{max}) observed in each kilometer of sample track was also determined. It should be noted that, because of infilling by sediment, the measured d values are presumably less than the d values at the time the gouge formed. It is also important to note that the gouge depth is almost always less than the depth to the base of the ice mass that produced the gouge, because of ploughed sediment sliding back into the gouge as soon as the keel moves on.

Maximum gouge width (w_{max}). This measurement was taken between the inside walls of the gouge at the level of the undisturbed surrounding sea floor (see Fig. 6); the maximum value in each kilometer of sample track was recorded.

Maximum lateral embankment height (h_{max}). This measurement is the maximum height (in each kilometer of sample track) of the embankments of sediment plowed from the gouges, measured relative to the undisturbed sea floor (see Fig. 6) and occurring along the margins of the gouges.

It should be noted that values of d and h_{max} are determined purely from the linear fathometer profiles. It is, however, known from other data (sonograms, dive observations, and repetitive tracklines) that both gouge depths and lateral embankment heights can vary considerably along the length of a given gouge.

Figure 5. Map showing the location of the sampling lines. Arrows indicate the direction of ship movement

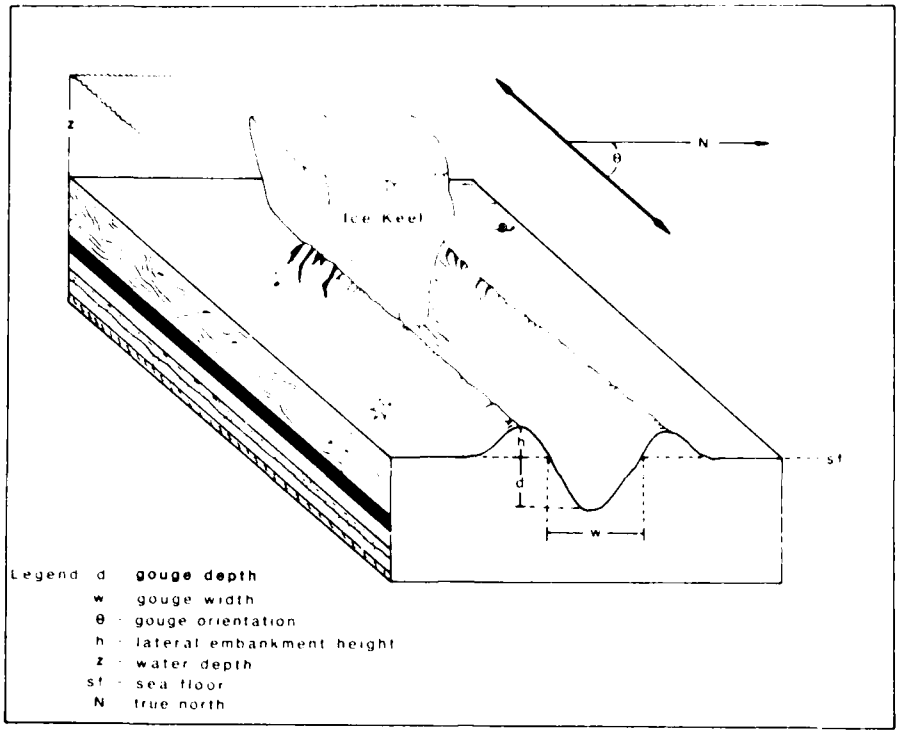

Figure 6. Schematic drawing of a gouge showing the locations of several measurements referred to in the text.

As is clear from comparing our terms with the titles of papers in our reference list, terminology for ice-induced sea floor features is far from standardized. This should not be a problem as long as individual authors clearly spell out their usage of specific terms. There is little we can do here to resolve terminology disputes. We would simply like to point out that gouge and gouging in the present study correspond to scour and scouring in the papers of Pelletier and Shearer (1972) and Lewis (1977a,b) and to score and scoring in the papers of Kovacs (1972) and Kovacs and Mellor (1974).

In the analysis the data are commonly combined into several different groups based primarily on geographic location. A given group is referred to by either a geomorphic characteristic common to the group or by the name of a geographic feature occurring within or near the location of the group. Specifically, the groups are:

a. Lagoons (lines 2-4, 14, 15; 3-7, 8, 9, 12, 13, 14; 5-3, 12; 8-37, 40, 41)
b. Lonely (lines 7-39, 40, 41, 42)
c. Harrison Bay (lines 2-19, 5-12, 6-22, 7-35; note that nearshore lines 6-20, 21, 23, 24, and 25 were not used, as the sonar records indicated sand waves and other features that suggested extensive movement of bottom sediment)
d. Jones Islands (lines 2-15, 17, 21, 7-31, 66, 67, 71; 9-92; observations from north of Spy Island to the north of the Midway Islands)
e. McClure Islands (lines 3-9, 10, 11, 13, 14; 5-3, 4; 7-76; 9-44, 63, 65, 66, 78; observations from Cross Island to Camden Bay)
f. Jones Islands and East (a combination of the Jones and the McClure Islands data sets; i.e. all the data seaward of the barrier islands and east of Harrison Bay)
g. Harrison Bay and East (a combination of the data sets from Harrison Bay, Jones Islands, and McClure Islands; i.e. all the data seaward of the barrier islands except the four tracks off Lonely).

DATA ANALYSIS

In the following five sections we will analyze our field results concerning a) gouge depths, b)

gouge orientations, c) gouge frequency, d) gouge widths, and e) lateral embankment heights.

Gouge depths

To examine the distribution of gouge depths, we prepared histograms of gouge depths for different regions. The general nature of these graphs appeared to be a decreasing exponential with a rapid fall-off in the frequency of occurrence of larger gouges. A similar tendency has been noted by both Lewis (1977a,b) and Wahlgren (1979a,b) for gouges occurring north of the Mackenzie Delta, but examination of this data (Lewis 1977a) shows that the number of small gouges is significantly less than would occur in an exponential model, suggesting that some other type of distribution might also be a possibility. As will be seen, this "non-exponential" decrease in the number of small gouges is not apparent in the data set studied in the present paper. We also note that the assumption of an exponential distribution of initial gouge depths is, as a first approximation, reasonable in that the depths of pressure ridge keels measured to the north of the study area by submarine sonar can also be well described by the use of an exponential distribution (Wadhams and Horne 1980).

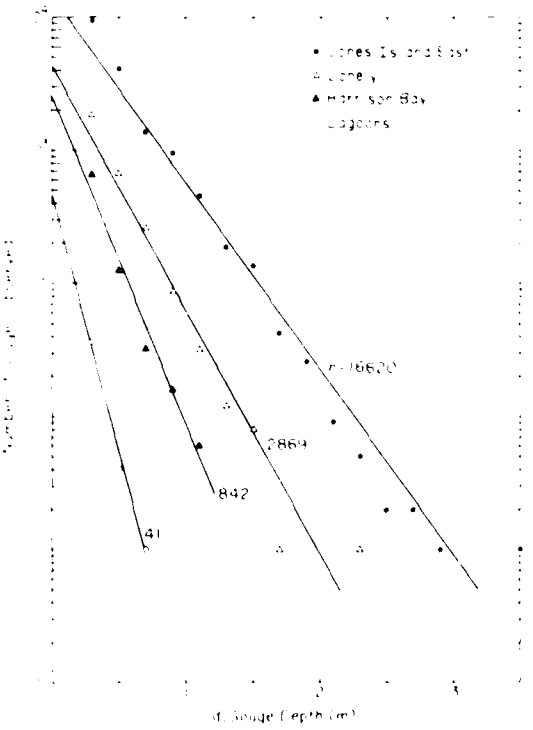

Figure 7. Semilog plot of the number of gouges observed vs gouge depth (d) for four regions along the Alaskan coast of the Beaufort Sea.

Figure 7 shows a semilog plot of the number of gouges with different gouge depths for four representative areas of the study region: 1) from the lagoons (41 data points), 2) from Harrison Bay (842 data points), 3) from off Lonely (2869 data points), and 4) from the profiles seaward of the barrier islands and east of Harrison Bay (16,620 data points). Other groupings of the data and data from other areas gave similar plots. The four curves are well separated because the number of gouges observed in the four regions are quite different. This is the result of differing lengths of sampling line and of differing spatial gouge frequencies associated with differences in water depth. If the same sets of data are plotted as relative frequency (the proportion of the total number of observations from that region that occurs in each of the 0.2-m depth classes), the shapes of the curves are identical but there is considerable overlap. Note that all plots are reasonably linear over the complete range of four decades (r^2 values vary from 0.94 to 0.98 [r^2 gives the fraction of the variation in the number of gouges observed accounted for by the regression line; in this case, 94 to 98%]). This suggests that the utilization of an exponential distribution in the Mackenzie studies (Lewis 1977a) is reasonable as an initial approximation. However we note that even though the correlation coefficients are high, χ^2 tests for goodness of fit are commonly failed. Future studies of gouging should explore the possibility of either finding a more satisfactory distribution function or of better rationalizing the deviations from exponentiality.

The exponential distribution is a convenient, well-studied distribution (see, among others, Benjamin and Cornell 1970, Miller and Freund 1977). If the simple frequency distribution is a negative exponential, then the probability density function (PDF) of X will also be of a similar form

$$f_X(x) = k e^{-\lambda x} \qquad x > 0.$$

(Here x represents the values that the random variable X may acquire.) Because the integral of $f_X(x)$ from 0 to ∞ must equal 1, as it contains all the sample points with non-zero probabilities,

$$\int_0^\infty k e^{-\lambda x} dx = \frac{k}{\lambda} e^{-\lambda x} \Big|_0^\infty = \frac{k}{\lambda} = 1$$

or

$$k = \lambda.$$

This gives the following PDF:

$$f_X(x) = \lambda e^{-\lambda x} \qquad x > 0. \tag{1}$$

Here the maximum likelihood estimate of the free parameter λ is simply the reciprocal of the sample mean ($\bar{x}$):

$$\hat{\lambda} = 1/\bar{x}.$$

The probability that a random variable will assume a value in the interval (x_1, x_2) is then

$$P[x_1 < X < x_2] = \int_{x_1}^{x_2} f_X(x)dx = \lambda \int_{x_1}^{x_2} e^{-\lambda x}dx.$$

The cumulative distribution function (CDF) is, in turn, found by integration

$$F_X(x) = P[X < x] = \int_0^x f_X(u)du = 1 - e^{-\lambda x}$$

where $x > 0$. Finally, because we are interested in the probability of occurrence of gouges that have depths greater than or equal to some specified value, we are largely concerned with the value of the exceedance probability given by the complementary distribution function $G_X(x)$

$$G_X(x) = P[X > x] = 1 - F_X(x) = e^{-\lambda x}. \tag{2}$$

$G_X(x)$ is a particularly simple function to graph as it is a straight line on semilog paper and has a value of 1 at $x = 0$. Therefore the simple relation

$$P[D > d] = \frac{n[D \geq d]}{N} = e^{-\hat{\lambda} d} \tag{3}$$

can be used to estimate $n[D \geq d]$ (the expected number of gouges with depths greater than or equal to d, given that N gouges have occurred). Values for $\hat{\lambda}$ for the four data sets shown in Figure 7 are given in Table 1a. In determining $\hat{\lambda}$ the fact that the 0 to 0.2-m gouge depth class was excluded was handled by letting $d' = (d - c)$ where $c = 0.2$ m, the cutoff value. (Note that in Figure 9 the nominal $d = 0$ location is, in fact, $d = 0.2$ m.)

Note also that *when the number of gouges is given, only gouges with depths equal to or greater than 0.2 m are counted.* The use of a cutoff has an undesirable effect on the estimates of the mean gouge depth in that the $\bar{d}$ value obtained depends upon the cutoff in use (in Table 1 the value $\bar{d}_{0.2}$ refers to a mean gouge depth calculated using the 0.2-m cutoff). To facilitate comparisons between our data set and those of other investigators we also include $\bar{d}$ values in Table 1 that are calculated by first estimating the number of gouges in the 0 to 0.2-m class interval by exponential extrapolation and then including this estimate in the calculation of the mean. The use of the resulting values, of course, implicitly assumes that the distribution of gouge depths is exponential. The values given in parentheses in Tables 1a and 1b for the 0.1-m class interval are the extrapolated values.

It is, however, possible to sharpen up the above by noting that, at least off the Mackenzie Delta, the nature of the gouge depth distribution is known to change with water depth (Lewis 1977a). This is hardly surprising in that the large ice masses that presumably produce the deep gouges observed in deeper water are not, because of grounding, available to produce similar gouges in shallow water.

We will now examine the effect of such a variation within our study area. That similar changes will be found to occur in the Beaufort Sea can be surmised from Figure 7 in that the shallower areas (lagoons, Harrison Bay) show no deep gouges. The $\hat{\lambda}$ and $\bar{d}$ values corresponding to various 5-m water depth classes in the different regions are given in Table 1a, and the $\hat{\lambda}$ values are plotted against water depth (z) in Figure 8. There is clearly a general decrease in $\hat{\lambda}$ with increasing z within the range of the data set.

For a discussion of the area in general, we have combined all the data for offshore areas unprotected by barrier islands (Lonely, Harrison Bay, Jones Islands and east) into one data set (Table 1b). Figure 9 gives three representative plots of data from this combined set for three different 5-m water depth intervals, and shows the fitted curves based on eq 1. Figure 10 shows the seven $\hat{\lambda}$ values for this combined set plotted versus $\bar{z}$. We have chosen to fit the $\hat{\lambda}$ vs z data with a negative exponential ($r^2 = 0.95$) purely as a matter of convenience. This curve should not be extrapolated beyond the range of the data. For instance, it is known (Lewis 1977a) that gouges off the Mackenzie Delta do not appear on the sea floor at water depths greater than 80 m and show a peak in the

Table 1. Summary of gouge depth (d) measurements.

Mid-point of class interval	A. All water depths				B. Lagoons			C. Lonely					D. Harrison Bay				E. Jones Islands and east					
	Jones Is. and east	Harrison Bay	Lonely	Lagoons	0-5 m	5-10 m	10-15 m	0-5 m	5-10 m	10-15 m	15-20 m	20-25 m	0-5 m	5-10 m	10-15 m	15-20 m	5-10 m	10-15 m	15-20 m	20-25 m	25-30 m	30-35 m
0.1	(10,176)	(1460)	(2535)	(189)	(59)	(289)		(441)	(1750)	(1151)	(917)	(488)		(444)	(759)	(515)	(115)	(497)	(3281)	(5415)	(3590)	(1304)
0.3	9401	646	1802	36	18	17	1	21	435	975	536	55	22	157	578	84	47	409	1685	4270	2427	764
0.5	4023	124	673	4	2	1	1	1	56	387	203	26		16	96	12	6	44	431	1661	1446	52
0.7	1378	32	253	1	1				4	156	93	2		5	25	2	4	12	91	426	604	24
0.9	957	16	87						3	45	39			2	14		1	2	46	250	482	126
1.1	453	6	32							15	17				7			2	17	93	252	85
1.3	188		12							5	7							2	4	41	94	47
1.5	135		8							5	3								2	24	72	44
1.7	42		1							1									1	4	23	13
1.9	26		0							0										5	12	10
2.1	9		0							0										3	5	1
2.3	5		1							1											4	1
2.5	2																				1	1
2.7	2																				1	1
2.9	1																				0	1
3.1	0																				0	
3.3	0																				0	
3.5	1																				1	
N	16620	824	2969	41	21	18	2	22	468	1590	696	95	22	180	512	105	58	475	2247	5485	5464	1964
$\bar{\lambda}$	3.47	6.13	4.59	7.7	7.24	9.00	5.00	9.17	7.62	4.51	3.54	6.08	10.0	7.58	5.46	7.63	6.83	7.10	5.25	4.47	2.98	2.29
$d_{0.2}$	0.47	0.36	0.42	0.5	0.54	0.51	0.40	0.51	0.55	.42	0.44	0.56	0.50	0.54	.54	0.55	1.56	0.54	.47	.42	.53	.57
$\bar{d}$	0.33	0.19	0.27	.14	0.16	0.11	0.33	.11	0.15	0.24	0.24	.18	.25	0.13	.21	.17	.14	.12	.21	.25	.33	.38
r^2	0.96	0.97	0.94	.99	0.92	1.00	1.00	1.00	0.95	1.97	1.00	0.93	1.00	.95	.96	1.00	0.96	1.00	.99	.99	.98	.99

Note: The $\bar{\lambda}$ values are calculated using $d = \lambda/20$ where 0.2 m defines the [illegible] of the d distribution. The r^2 [illegible] value (given in parentheses) for the [illegible] interval (see text).

Table 1 (cont'd). Summary of gouge depth (d) measurements.

Midpoint of class interval	All regions (C+D+E) excluding B. Lagoons						
	0-5 m	5-10 m	10-15 m	15-20 m	20-25 m	25-30 m	30-35 m
0.1	(1849)	(2196)	(1953)	(5273)	(7006)	(3390)	(1460)
0.3	43	609	1761	2110	4135	2427	764
0.5	1	78	532	616	1587	1486	520
0.7		13	196	184	428	604	241
0.9		6	61	85	250	482	176
1.1			24	34	93	252	86
1.3			7	11	41	94	47
1.5			5	5	28	72	35
1.7			1	1	8	23	10
1.9			0		3	12	11
2.1			0		3	5	1
2.3			1			4	1
2.5						1	1
2.7						1	1
2.9						0	1
3.1						0	
3.3						0	
3.5						1	
N	44	706	2588	3046	6576	5464	1893
$\underline{\lambda}$	9.57	7.43	5.03	5.09	4.48	2.98	2.73
$d_{0.2}$	0.30	0.33	0.40	0.40	0.42	0.54	0.57
$\overline{d}$	0.10	0.16	0.27	0.21	0.26	0.37	0.36
r^2	1.00	0.97	0.92	0.99	0.99	0.94	0.95

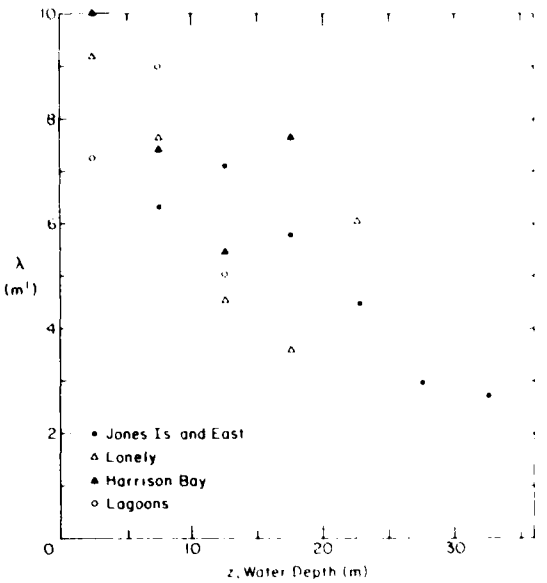

Figure 8. Plot of λ (m^{-1}) vs water depth (z) in meters for four geographic areas along the Alaskan coast of the Beaufort Sea.

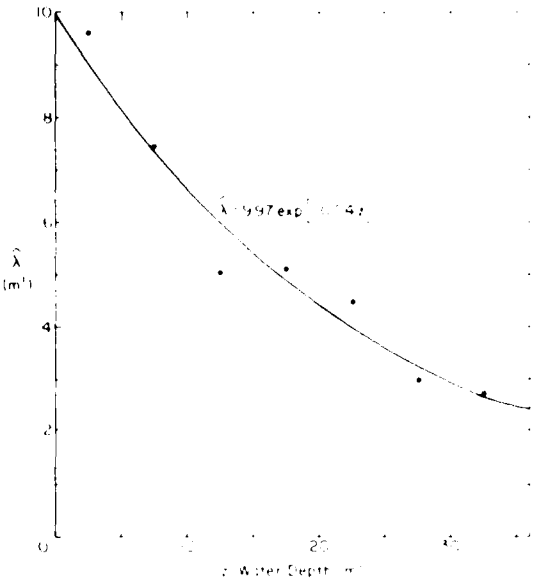

Figure 10. λ values (m^{-1}) vs water depth (z) based on the data set from offshore areas unprotected by barrier islands.

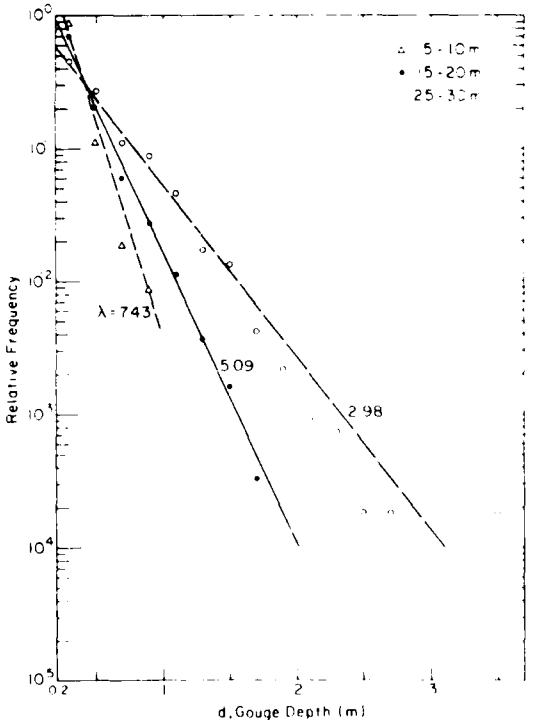

Figure 9. Relative frequency of occurrence of gouges of differing depths based on all data from offshore areas unprotected by barrier islands.

mean gouge density at a water depth of 23 m. Therefore, one might expect that in the present study area $\hat{\lambda}$ values may increase again at $z > 35$ m.

Clearly, water depth is a most important parameter in studies of gouging.

Gouge orientation

Determining the absolute cartographic orientation of every gouge would be very time-consuming. To provide some information on gouge orientations we have visually estimated the dominant orientation that exists along each kilometer of sample track. These orientation values, however, do not provide information on the actual direction of the ice movement; for instance, the direction 90° indicates only that the gouge runs along the 90° to 270° line (in an east-west direction).

Figure 11 shows linear histograms of the probability of the occurrence of different orientations. The data are displayed between 0 and 180°. This proved to be convenient, as there was a natural break in the observations at this orientation (i.e. very few gouges were aligned north-south). Summary statistics for these observations are presented in Table 2. The mean given here is the circular mean as calculated for axial data; the circular variance has a value near 0 if the data are tightly clustered and a value near 1 if the directions are

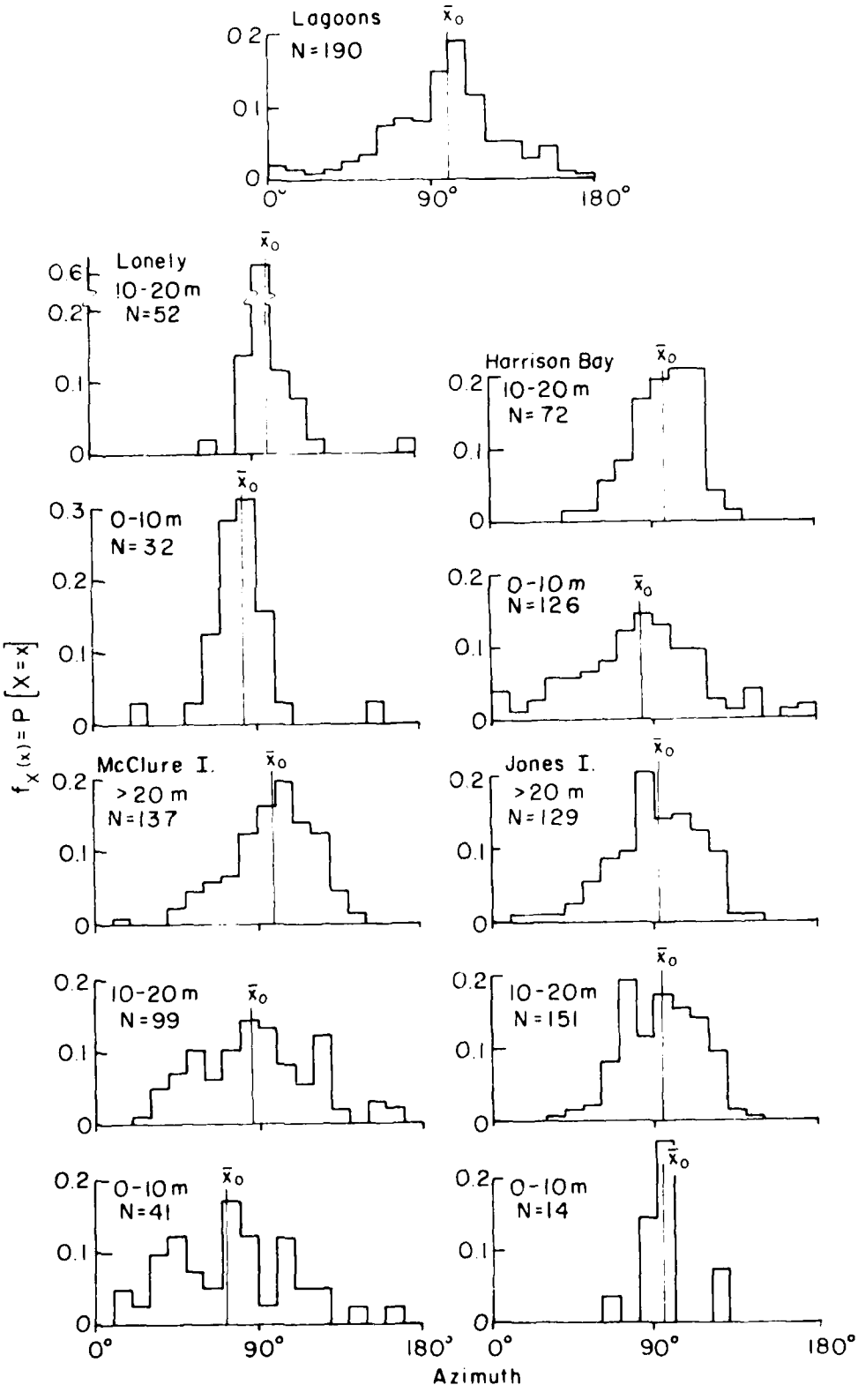

Figure 11. Linear histograms of the observed probability of dominant gouge orientations.

Table 2. Descriptive statistics on variations in the dominant gouge orientation.

Location	*Water depth range (m)*	*Sample size N*	*Mean direction $\bar{x}$ (degrees)*	*Circular variance S*	*Standard deviation s (degrees)*
Lagoons	all	190	99.2	0.142	15.9
Lonely	0–10	32	80.3	0.045	8.7
	10–20.4	52	96.6	0.023	6.2
Harrison Bay	0–10	126	82.7	0.162	17.0
	10–20	72	97.4	0.047	8.9
Jones Island	0–10	14	93.8	0.032	7.4
	10–20	151	94.0	0.066	10.6
	>20	129	92.3	0.081	11.8
McClure Islands	0–10	41	71.6	0.169	17.4
	10–20	99	86.4	0.149	16.3
	>20	137	99.0	0.080	11.7

widely dispersed; the standard deviation is somewhat analogous to the ordinary standard deviation on a line (Mardia 1972, pp. 18–27).

Figure 11 and Table 2 show several obvious features. First, the dominant gouge orientations appear to have a unimodal distribution that is reasonably clustered. Second, gouge orientations show more variability in the lagoons and in other shallow water (0–10 m) areas. Farther off the coast in deeper water, these variations generally decrease (increased clustering; lower S_0 and s values). The average orientation in water deeper than 20 m is 97° to 99° T, which is just a few degrees less than parallel to the coast (110° T). In shallow areas the gouges generally show a higher angle (71° to 83° T) to the coast, although this tendency is not evident in the measurements made off the Jones Islands. It is reasonable to expect a grounded floe to rotate and move toward the coast (this effect has been observed in radar imagery at Barrow by Shapiro [pers. comm.]). However, it is not clear to us why this phenomenon should be more pronounced in shallow water. The mean gouge orientation in the lagoons is 99° T, which is similar to the gouge orientations in water deeper than 20 m.

Three factors presumably control the orientation of the gouges. The first factor is the wind direction, which at Kaktovik is predominantly in two directions: from the ENE-E (55°–100° T) 35% of the time and WSW-W (235°–280° T) 23% of the time (the mean wind speed is the same [6.7 m/s] in both directions [APO 1978]). Therefore the ice drift, which is roughly 45° to the right of the surface wind, would be expected to be between 100° and 145° T, a value range just above that observed. Secondly, because the fast ice edge generally parallels the isobaths, ice-ice interactions tend to force the near-shore ice to drift parallel to the coast even when the free-drift direction is not exactly parallel with the coast.

Finally, as mentioned, the higher resistance commonly encountered by grounded features on the near-shore (shallow water) side of a floe will cause gouges to form at angles less than expected from a free-drift situation. The end result is therefore an average gouge direction in the range of 80° to 125° T, as observed.

Gouge frequency

We now have a reasonable description of the probability of a gouge having different gouge depths, given that a gouge has occurred. Next we need to determine how many gouges have occurred so that we can estimate N in eq 3. The number of gouges that is of primary interest is the temporal gouge frequency, that is, the number of gouges that intersect a unit length of line per unit of time (gouges per kilometer per year). As will be seen, data leading to such estimates are extremely sparse. What is available are measurements of the spatial gouge frequency (e.g. gouges per kilometer) as seen at a given location at essentially a fixed instance in time. We will now discuss these two parameters.

Spatial gouge frequency

To study variations in the spatial gouge frequency, the number of gouges deeper than 0.2 m per kilometer was determined for each kilometer

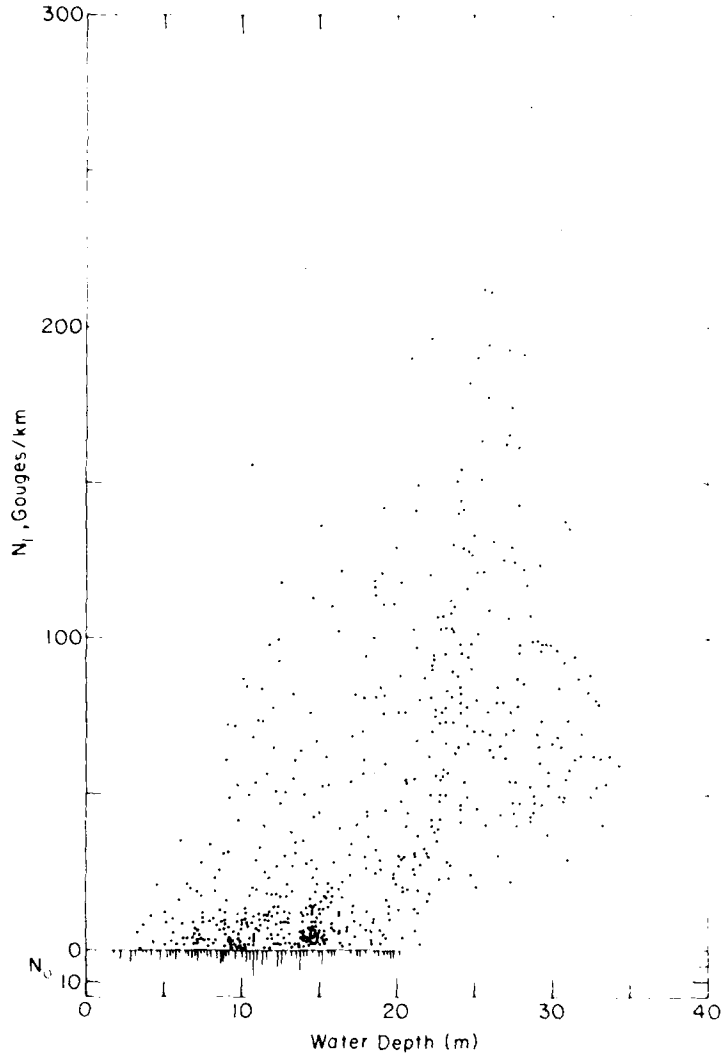

Figure 12. Number of gouges per kilometer measured normal to the trend of the gouges (N_i) vs water depth (z).

of sampling track. These values were then converted to N_i, the number of gouges per kilometer that would have been encountered if the sampling track were oriented perpendicular to the trend of the gouges. The values were then separated into five different groups (lagoons, Lonely, Harrison Bay, Jones Islands, and McClure Islands and east) and plots were made of N_i vs water depth. Examination of these plots showed that lagoons differed from the other four areas in that gouges were rare (92% of the 298 kilometers sampled contained no gouges and the largest N_i value was 12 gouges/km). The four other regions showed differences but these appeared to be largely caused by changes in the water depths sampled in the different areas. Therefore all four regions were combined and considered as one. Figure 12 shows the N_i vs z plot for the combined data. A data tabulation is presented in Table 3. As was the case in the lagoons, in shallow water N_i values of zero (N_0 values) are common and N_i values greater than 50 are rare. In water 15 to 20 m deep, zero values become less common and larger N_i values are encountered. Finally, as water depths increase above 22 m, all samples show 20 or more gouges per kilometer.

These changes can be shown (Fig. 13) by taking 10-m-wide vertical slices through Figure 12 and

Table 3. Summary of the number of gouges per kilometer deeper than 0.2 m.

N Number of gouges deeper than 0.2 m per kilometer	Frequency of occurrence (lagoons)	$N_i/10$ Number of gouges deeper than 0.2 m per 100 m	Frequency of occurrence Offshore 0–10 m	all sites but lagoons 10–20 m	20–38 m
0	275	0	62	88	1
1	7	1	67	154	5
2	8	2	10	31	13
3	4	3	5	20	15
4	0	4	2	12	19
5	2	5	2	12	27
6	1	6	1	9	21
12	1	7	2	7	23
	$N = 298$	8	$N = 151$	10	26
		9		4	16
		10		4	21
		11		5	8
		12		5	9
		13		0	9
		14		2	7
		15		0	4
		16		1	3
		17		0	2
		18		0	2
		19		0	5
		20		0	3
		21		0	0
		22		1	0
		23		$N = 365$	2
		24			0
		25			0
		26			0
		27			1
					$N = 242$

displaying the results as histograms giving relative frequency vs $N_i/10$. As can be seen, in the lagoons there is a rapid exponential drop-off in frequency as the $N_i/10$ value increases. In shallow water (<10 m) outside of the barrier islands the trend is similar, although null values are not as frequent (42%). At depths of 10 to 20 m, the null values compose only 24% of the total sample and $N_i/10$ values in excess of 10 are not rare. In deeper water the distribution from 20 to 30 m and 30 to 38 m had nearly identical means and forms and were therefore combined. The histogram is now more clearly Gaussian and shows only a slight positive skew. Again, the nature of the distribution is clearly a function of the water depth. One additional piece of information should be added here: at one location (off Lonely) a study was made of the distribution of the spacings between the centers of gouges (as measured along the sampling line); the distribution resembled a negative exponential (Fig. 14).

It would be convenient to have one distribution function that would describe all the histograms shown in Figure 13. If possible this distribution should have the following characteristics:

a. It should be discrete in that we are describing a counting process (either a gouge is present or it is not)
b. It should be capable of dealing with a positive frequency of zero values
c. It should have a shape that varies from a negative exponential to normal as the mean value of N_i increases
d. The distribution of spacings between occurrences should be given by the exponential distribution.

The Poisson distribution has, in fact, all these characteristics and is given by

$$f_X(x,\alpha) = \frac{\alpha^x e^{-\alpha}}{x!} \qquad (4)$$

$$x = 0,1,2,3,\ldots; \qquad \alpha > 0$$

where the parameter α is the sample mean, which in our case varies from 0.08 for lagoons to 8.07 for depths in excess of 20 m. As we have plotted $N \leq 10$, these sample means correspond to N values of 0.8 and 80.7 gouges km^{-1}. The use of $N \leq 10$ was necessitated by the fact that N values as large as 270 gouges km^{-1} occur. The Poisson distribution, on the other hand, is not convenient for values much in excess of 20. When $N \leq 10$ is used, the Poisson probability for an integer such as 3 is used to represent the probability of N occurring in the interval $2.5 \leq N \leq 3.5$ gouges per kilometer. Examination of Figure 13 shows that the Poisson distribution (the discrete values) does, in fact, give a reasonable representation of the frequency plots of the N values, although it drops off too rapidly at large $N \leq 10$ values. The Poisson distribution also possesses the additive property that the sum of two independent Poisson random variables with parameters α_1 and α_2 is also a Poisson random variable with parameter $\alpha = \alpha_1 + \alpha_2$.

The use of the Poisson distribution brings to mind its association with the Poisson process, describing the frequency of random events occurring *at a constant rate along a continuous space* (or time) scale. To be a Poisson process, the underlying physical mechanism generating the events must satisfy the following three assumptions:

1. *Stationarity*—The probability of at least one event in any short interval is proportional to the length of the interval.
2. *Nonmultiplicity*—The probability of two or more events in a short interval Δx is negligible in comparison to $\alpha \Delta x$.
3. *Independence*—The number of events in any interval is independent of the number of events in any non-overlapping interval.

The probability distribution of the number of events N in distance x for a Poisson process is given by

$$f_N(n; \nu x) = \frac{(\nu x)^n e^{-\nu x}}{n!} \qquad (5)$$

$$n = 0,1,2,3,\ldots; \qquad \nu x > 0$$

where νx has replaced α in eq 4 and parameter ν is the average spatial rate of occurrence of the event.

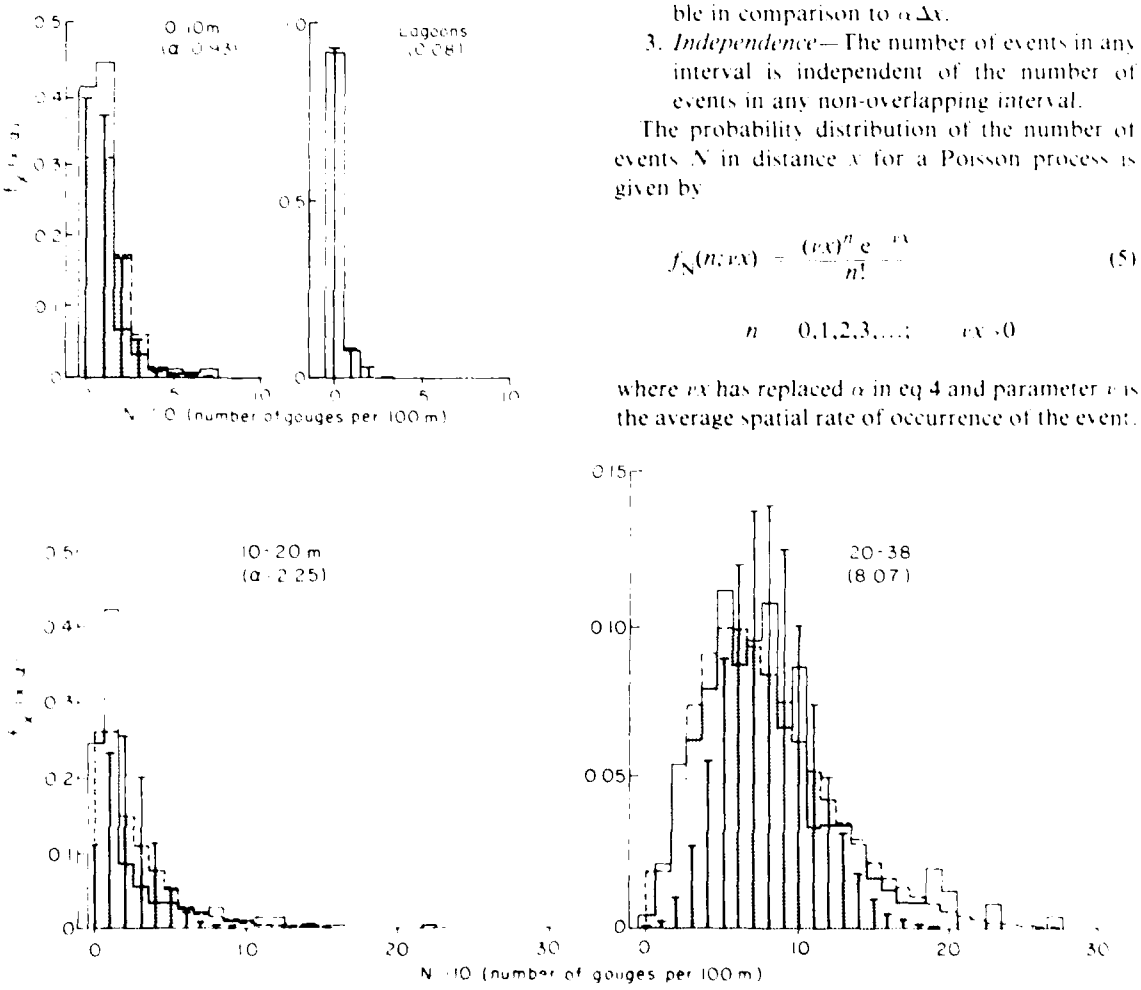

Figure 13. Relative frequency of different $N \leq 10$ *values for lagoons and three different water depth ranges offshore of the barrier islands. The solid line bar graph represents the data, the discrete values indicate the fitted Poisson distribution, and the stippled area indicates the fitted gamma distribution.*

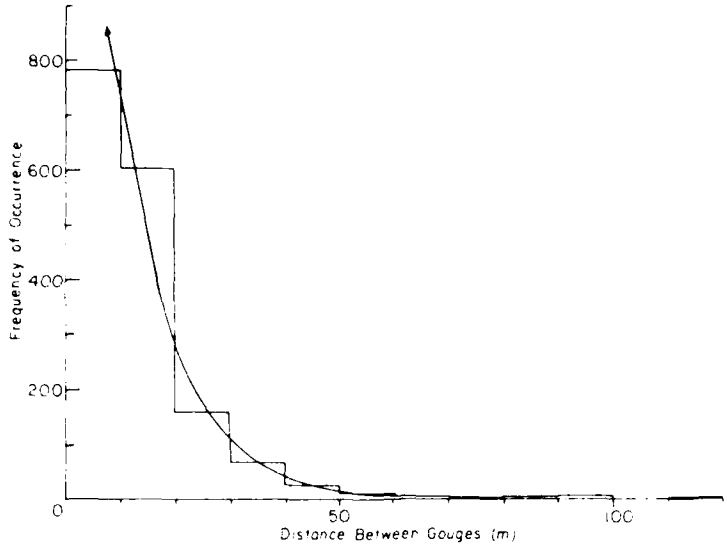

Figure 14. Frequency of occurrence vs observed distances between the gouges off Lonely, Alaska.

We would judge that, when gouging is looked on as an annual event, it would satisfy the requirements for a Poisson process reasonably well as a first approximation. We note however that when the spatial distribution of gouging is examined in more detail it is found that there are locations where gouges occur in groups (on the seaward sides of shoals, for example). In addition, if gouging is examined on a time scale finer than yearly, the assumption of stationarity is clearly not satisfied, since in many locations no gouging occurs during the summer months. However, these problems are probably no worse than in many other areas, such as customer arrivals and number of telephone calls per unit time, where the Poisson process has been found to be a very useful model.

It is, of course, possible to use other distribution functions, such as a gamma distribution. This distribution is attractive for several reasons. First, it is capable of assuming shapes similar to those shown in Figure 13 (Hahn and Shapiro 1967, Figures 3-7b and 3-8). It is also an applicable distribution to data such as N_i that are bounded on one end (however it is not capable of treating the occurrence of zero values). In addition, this distribution has been used successfully in a variety of engineering problems because of its flexibility (Benjamin and Cornell 1970). The gamma distribution is given by

$$f_X(x) = \frac{\lambda^{\eta} x^{\eta-1} e^{-\lambda x}}{\Gamma(\eta)} \tag{6}$$

$$x \geq 0, \ \lambda > 0, \ \eta > 0$$

where $\Gamma(\eta)$ is the gamma function

$$\Gamma(\eta) = \int_0^{\infty} x^{\eta-1} e^{-x} dx. \tag{7}$$

Here the two free parameters η and λ can be considered to be shape and scale parameters respectively. The mean, variance, and coefficient of skew for the distribution are respectively

$$E(x) = \eta/\lambda \tag{8}$$

$$\mathrm{Var}(x) = \eta/\lambda^2 \tag{9}$$

$$\gamma = 2/\sqrt{\eta}. \tag{10}$$

The exponential distribution is, in fact, a special case of the gamma distribution with $\nu = 1$.

As can be seen in Figure 13, the gamma distribution (the dashed lines) gives a very reasonable representation of N_i data if the presence of zero values is arbitrarily introduced in calculating the

Table 4. Parameters of gamma distributions fitted to observational data on spatial gouge frequency. For the combined offshore data set, the data are expressed in terms of the number of gouges per kilometer (10).

Lancaster	Nordegg	298	23	Contact	100%	2.555	0.785	2.136	4.474	96
Canmore–Exshaw	0–10	151	82	Contact	100%	2.509	3.542	574	1.853	7
Canmore–Exshaw	10–20	365	255	Contact	100%	2.296	0.436	2.972	6.826	747
data set	20–38	242	243	Contact	100%	3.023	0.373	8.105	21.729	1.000

appropriate probabilities. Note that the gamma distribution is more successful in fitting the larger N 10 values than is the Poisson distribution, which drops off too quickly at large values of N 10. Table 4 gives the values of the parameters of the fitted gamma distributions. The λ and η values were obtained using the maximum likelihood procedure suggested by Thom (see Haan 1977, pp. 102–106). In comparing the Poisson and the gamma mean values it should be remembered that the Poisson mean includes the effects of the presence of zero N values while the gamma mean does not.

Temporal frequency

In investigating problems concerning ice-induced gouging of the sea floor it is highly desirable to have independent information on the rates

Table 5. Number of new gouges during the indicated time and space intervals. (Determined from replicate sonar data collected during the summers of the years indicated.)

Interval	*Test line 35*					*Test line 37*			*Test line 39*	
(m)	*x (m)*	*1973–75*	*1975–76*	*1976–77*	*1977–78*	*x (m)*	*1975–76*	*1976–77*	*x (m)*	*1977–78*
0–1	5.9				0	8.9	3	1	4.2	0
1–2	7.5			1	15	11.0		1	5.8	0
2–3	8.0	2	5	6	9	11.7	2	1	7.1	0
3–4	9.0			5	0	12.0		6	8.4	0
4–5	9.8	4.5	5	8	3	13.0	5	5	9.4	0
5–6	10.0			11	9	14.0		1	10.2	0
6–7	10.1	0	3	2	1	14.8	3	5	10.9	0
7–8	10.6			7	3	15.0		5	11.6	2
8–9	11.2	1	10	5	4	14.6	1	4	12.4	5
9–10	11.8			0	19	15.1		2	13.3	0
10–11	12.5	0.5	6	6	4	15.8	10	1	14.0	5
11–12	13.0			7	3	16.3		2	14.6	13
12–13	13.3	1	8	7	12	17.2	8	4	15.0	0
13–14	13.7			9	33	18.0		1	15.5	12
14–15	14.2	1.5	3	2	13	18.5	9	4	16.3	52
15–16	14.5			0	11	19.0		2	17.1	27
16–17	14.8		1	2	11	19.4		0	17.9	7
17–18	15.1			3		19.8		1	18.5	11
18–19	15.4		4	–	–	20.3		1	18.9	9
19–20	15.6			–					19.3	0
20–21	15.8			–					19.7	1
21–22	16.0			–	21				20.1	6
22–23	16.3		6	1	3				20.3	0
23–24	16.5			4	9				20.4	0
24–25	16.5			2					20.2	0
25–26									19.2	0
26–27									17.9	2
27–28									17.3	0
28–29										0
$\bar{g}$		0.4	2.1	4.4	9.2		1.1	2.5		6.8

Note: The 1973–75 and 1975–76 data are from Barnes et al. (1978).
The symbol – indicates no data was collected.
Also given are values of $\bar{g}$, the average number of new gouges per kilometer per year.

at which new gouges form (the number of new gouges per kilometer per year). Unfortunately such data are rather limited; for our study area they are largely contained in a paper by Barnes et al. (1978). This work describes replicate observations made on sample line 35 (see Fig. 5 for location) during the summers of 1973, 1975, 1976, and 1977 and on line 31 during the summers of 1975, 1976, and 1977. We have reanalyzed the data set from line 31 for 1976–77 and on line 35 for the 1976–77 and 1977–78 intervals so that the counts of new gouges are based on 1-km sampling lines. We have also analyzed replicate runs on line 39 (north of Cape Halkett) for 1977–78.

Because the quality of the 1973 sonar records was poor (Reimnitz et al. 1977a), data based on the 1973–75 time interval should receive less weight than the later observations. The results of this analysis and that of Barnes et al. (1978) are combined and presented in Table 5. We have arbitrarily deleted the $\bar{g}$ values obtained on line 39 at 20.3 m and farther offshore, since this portion of the line is known to be in the shadow of a nearby shoal area, thereby receiving fewer gouges. If the 1973–75 data on test line 35 are also excluded because of the poor quality of the sonar record, we obtain an average $\bar{g}$ value of 5.2 gouges per kilometer per year with values for individual years varying from 2.4 (1975–76) to 3.5 (1976–77) to 7.9 (1977–78). These are appreciably larger values than have been obtained using similar procedures off the Mackenzie Delta in 15 to 20 m of water (0.19 ± 0.06 gouges per kilometer per year, Lewis 1977a) and they give a return period per kilometer of 0.2 years as compared to 5.3 years.

Figure 15 shows a plot of observed $\bar{g}$ values vs water depth. There is no strong trend. In addition, there is a large scatter and zero values (1-km lines with no new gouges) are rather evenly distributed at all water depths. Because of this we have treated all the observations as a single group.

Figure 16 shows a plot of the observed probability of occurrence of different values of $\bar{g}$. The distribution shows a strong positive skew. The Poisson distribution for this set of data is also shown. The representation of the data is not encouraging (again the probability of occurrence falls off much too rapidly at large $\bar{g}$ values). Also shown is a gamma distribution, which gives a better fit (the shape and scale parameters are respectively η = 1.205 and λ = 0.196).

While the characteristics of the new gouges are being discussed, it is of interest to examine the distribution of their depths to see if they appear to follow an exponential distribution similar to that obtained by sampling all the gouges on the sea floor, a data set that contains a number of old gouges that presumably have been partially filled with sediment as well as new unfilled gouges. The observations used (n = 76) were from both test lines 31 and 35 and occurred between 1976 and

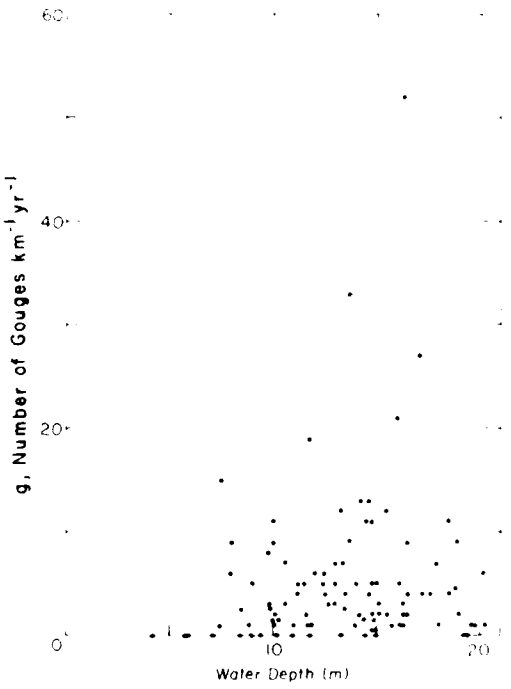

Figure 15. Values of $\bar{g}$ (number of gouges km^{-1} yr^{-1}) vs water depth (z).

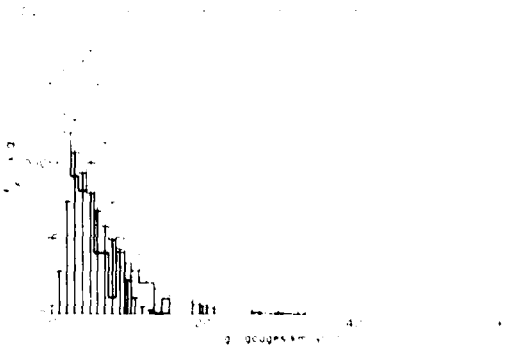

Figure 16. Relative frequency of different values of $\bar{g}$ (number of gouges km^{-1} yr^{-1}). The discrete values indicate the fitted Poisson distribution and the stippled area indicates the fitted gamma distribution.

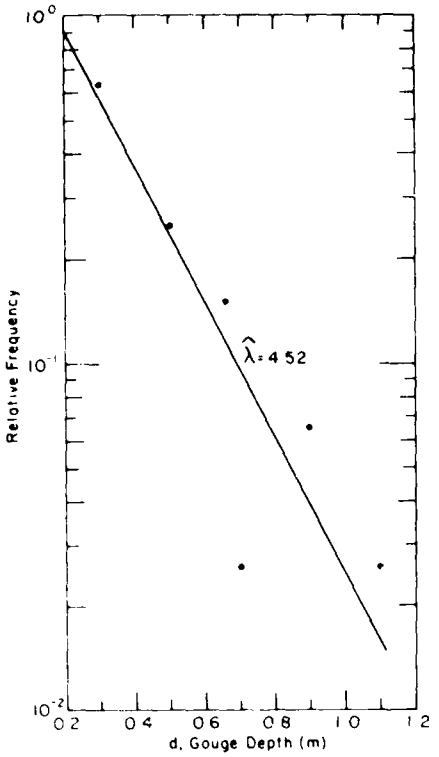

Figure 17. Semilog plot of relative frequency of occurrence of new gouges of differing depths (d).

1977. The results are shown in Figure 17. Again the data appears to show an exponential dropoff with a $\hat{\lambda}$ value of 4.52 m^{-1}. This value is close to but somewhat lower than the values obtained from the samples of all the gouges (taking 15 m as a mean water depth along the replicate sampling lines, we obtain a value of 5.5 m^{-1} from Figure 10, as contrasted with 4.5 m^{-1} from the new gouges). That new gouges should have a lower λ value than a corresponding distribution of old and new gouges could be anticipated (E. Phifer, pers. comm.) from the observation that at other locations deep gouges in the sea floor receive more fill per year than do shallow gouges (Fredsoe 1979). At the present there clearly is no strong reason to doubt that the distribution of new gouge depths is exponential or that the λ values that will be obtained are greatly different (presumably slightly less) than values obtained from our earlier analysis of all the gouges.

Extreme value analysis

Another way to view portions of the gouging data is by extreme value analysis. In this case the complete data set is not examined. Instead the largest (or smallest) value in each of a number of specified sampling intervals is used. In most applications, such as hydrology, the data are in the form of time series, and the largest (smallest) event in each of a sequence of fixed time intervals is used to generate a distribution of rare events. In our study, the basic data set is a space series, as separate frequency distributions of gouge characteristics were developed for each kilometer of sampling line. For instance, in a kilometer of line one might observe 85 gouges of different depths, with the largest gouge having a value of 2.2 m; in the next kilometer there might be 178 gouges with a maximum value of 3.1 m. The extreme value distribution would then be composed of the values 2.2, 3.1, and subsequent values. Good discussions of the different types of extreme value distributions can be found in Hahn and Shapiro (1967), Benjamin and Cornell (1970) and Haan (1977).

The particular extreme value distribution applicable to a given situation depends on the nature of the initial distribution being sampled and on the sample size n, with the extreme distribution being approached asymptotically as n becomes large. A common problem is that many times n does not appear to have been large enough, and the extreme value distribution that would be expected to apply to a given data set is not particularly successful in fitting it. For instance, a Type I extreme value distribution should apply to maximum values sampled from an initial distribution that is of the exponential type. However, Tucker et al. (1979), in their study of maximum pressure ridge heights whose initial distribution appears to be the exponential type, found that their data were not linear on Type I paper but were effectively linearized by standard probability paper. Similar results have been obtained by other workers in hydrology and in Monte Carlo simulations by Slack et al. (1975). In practice, a number of different approaches (Type I, normal, log-normal, log-Pearson Type III) are commonly tested, and the most successful relation is selected to analyze the data.

Gouge depths

As we have shown, gouge depths appear to be exponentially distributed. Therefore, the appropriate extreme value distribution for maximum

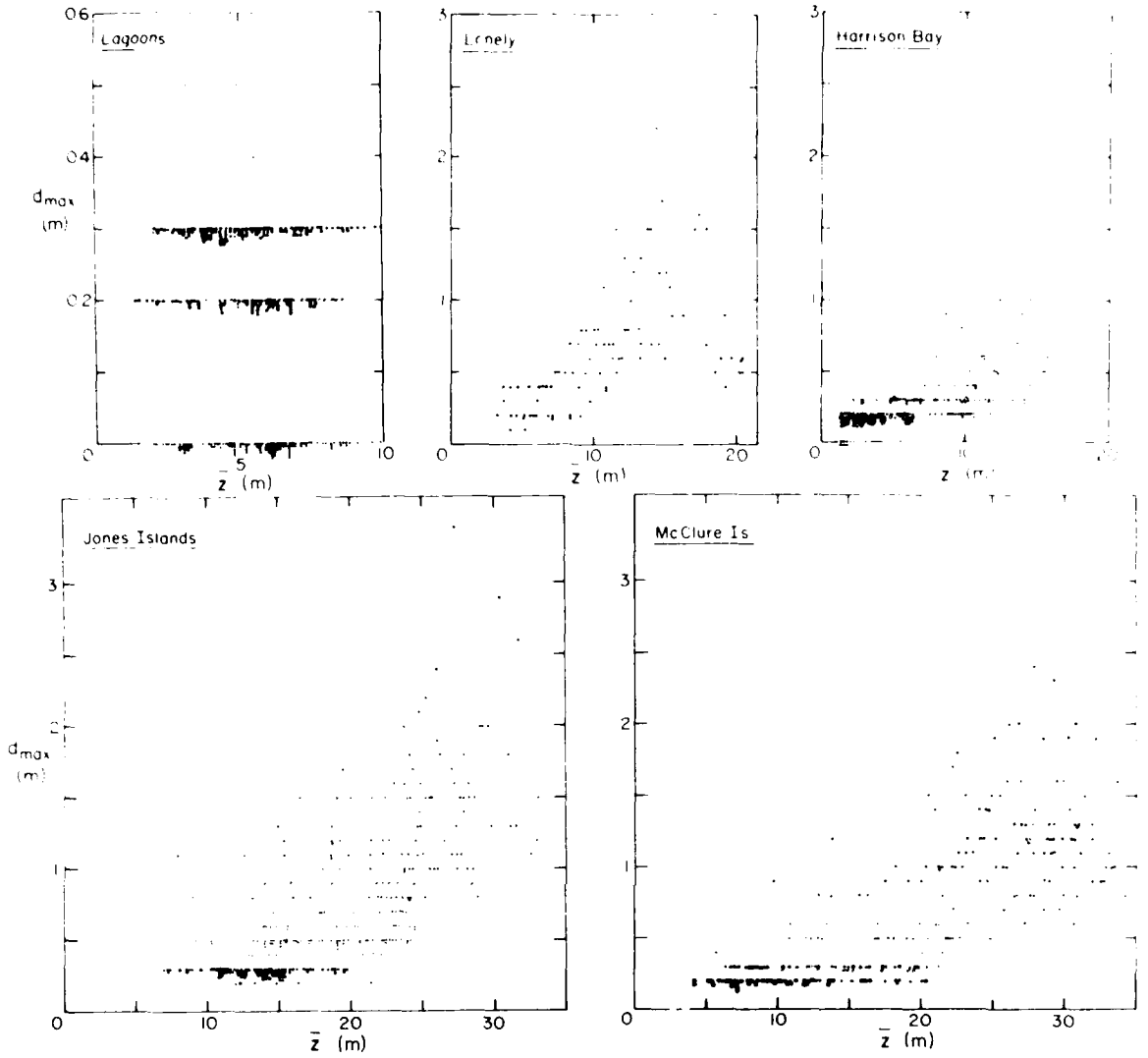

Figure 18. Plots of d_{max} vs water depth ($\bar{z}$) for different regions within the study area.

gouge depths should be a Type I distribution. However, testing shows that the data were not linearized by either a Type I, a normal, or a log-normal distribution. However, a log-Pearson Type III (LPIII) distribution proved to be quite effective. This distribution, which is in fact a three-parameter gamma distribution fitted to the $\log_{10}$ of the extreme values, has been used successfully in treating flood observations (USWRC 1977). The three parameters describing an LPIII distribution are the mean $\bar{X}$, the standard deviation S, and the skew coefficient G, which, if $X \equiv \log_{10} d_{max}$, where d_{max} is the maximum gouge depth in a kilometer track and N is the number of maximum gouges, are calculated as follows:

$$\bar{X} = \frac{\Sigma X}{N}$$

$$S^2 = \frac{\Sigma(X - \bar{X})^2}{N - 1}$$

$$G = \frac{N\Sigma(X - \bar{X})^3}{(N-1)(N-2)S^3} .$$

The computed d_{max} value is then given by the relation

$$\log_{10} d_{max} = \bar{X} + KS \qquad (11)$$

where K is the Pearson Type III coordinate expressed in magnitudes of the standard deviation

from the mean for various exceedance percentages. Values of K are functions of G and are given in Appendix 3 in USWRC (1977), as are the computing equations for $\bar{X}$, S, and G.

In analyzing the d_{max} values on gouging, individual plots (Fig. 18) were prepared showing d_{max} vs $\bar{z}$ for five different areas. The different regions were compared by overlaying the figures on a light table. If differences in water depth are taken into consideration, the data from Lonely, Harrison Bay, Jones Islands, and McClure Islands overlap very well and appear to form one continuous distribution. Therefore, as before, the data were pooled into one sample. The data from the lagoons were treated separately, both because they appear different and they represent a different marine environment.

Another characteristic of the d_{max} data, which might be anticipated from our earlier discussion and that is apparent in Figure 18, is that the values clearly change with water depth. There are null values, many small values, and no large values in shallow water; large values of d_{max} become increasingly common with increasing z; and small values are rare in water deeper than 20 m. Therefore, as before the pooled offshore d_{max} data were separated into 5-m water depth increments. As no similar z trend was apparent in the data from lagoons and, as the depth range was limited, these results were not separated into similar groups.

In analyzing the data, two problems were encountered. First, in a number of shallow water areas we commonly found appreciable lengths of track that did not contain gouges, resulting in $d_{max} = 0$ values. For instance, in the data set for lagoons, 119 km of the 324 km sampled (37%) were gouge-free. This precludes the normal statistical analysis of the data using an LPIII distribution, as the $\log_{10}$ of zero is minus infinity. Secondly, in a number of cases it was impossible to determine precisely the depth of the smaller gouges, only that a gouge existed and that its depth was less than some specified value. Such gouge depths are identified by circles in Figure 18. In most cases they had values of less than 0.3 m and were situated in shallow water. This created considerable uncertainty in specifying the exact number of gouges in the 0.1- and 0.2-m depth classes. Where such gouges were common (at water depths of less than 10 m), large G values and LPIII distributions were obtained that were not particularly good fits to the data at the larger d_{max} values (which, of course, is the area of prime interest).

Both of these problems were handled using a procedure developed for treating zero flood years and incomplete records in hydrology. First, the 0, 0.1-, and 0.2-m values were deleted from the samples. Then the $\bar{X}$, S, and G parameters were calculated from the censored distributions and used to calculate d_{max} as a function of exceedance probability. These exceedance probabilities were then adjusted by multiplying them by the ratio of the number of values in the censored distribution to the number of values in the uncensored distribution (i.e. with the 0, 0.1, and 0.2 values included). The results were then plotted on log-probability paper for comparisons with the observed data. In plotting the data against the adjusted curve, the plotting positions were determined by using the Weibull plotting formula

$$P = m/(N+1)$$

where P is the exceedance probability; m the sequence of d_{max} values, with the largest values corresponding to $m = 1$, the next largest value corresponding to $m = 2$, etc.; and N the total number of data points before censoring (i.e. including 0, 0.1, and 0.2 values).

Table 6. Parameters of the log-Pearson Type III distribution (determined from values of d_{max} observed along 1-km sampling lines. Values outside the barrier islands include data from Harrison Bay and north of Lonely.

Depth (m)	Number of values $d_{max} < 0.3$	Number of values $0.3 < d_{max} > 0$	$d_{max} = 0$	Sample line length (km)	Largest d_{max} value	$\log d_{max}$ $\bar{X}$	Standard deviation S	Skew coefficient G	Exceedance factor K
Lagoons	13	192	119	324	0.6	0.4232	0.1231	0.6909	0.040
Outside barrier islands									
0–5	3	65	11	79	0.4	0.4812	0.0721	1.7305	0.038
5–10	54	88	0	142	1.1	0.3466	0.1609	0.5508	0.380
10–15	146	69	0	215	2.2	0.2623	0.2091	0.4141	0.679
15–20	104	38	0	142	1.7	0.2282	0.2070	0.3345	0.732
20–25	128	3	0	131	2.1	0.0933	0.1942	0.0908	0.977
25–30	81	0	0	81	3.6	+0.1095	0.1502	0.3236	1.000
30–35	35	0	0	35	2.9	+0.0964	0.1466	0.427	1.000

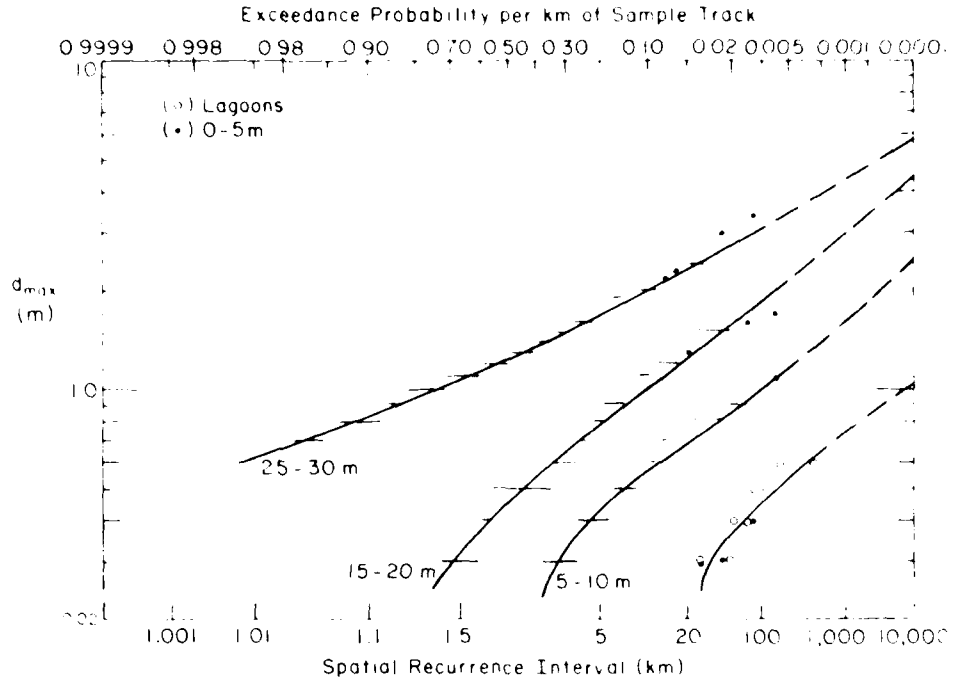

Figure 19. Exceedance probability per km of sample track for different water depths vs d_{max}. The horizontal lines represent the locations of a number of data points (as the data are grouped in class intervals there commonly are several values of the exceedance probability with the same d_{max} [midpoint of the class interval] value).

Table 6 gives the $\bar{X}$, S, and G values calculated from the different sets of censored data as well as the adjustment ratio and the number of d_{max} values equal to zero and between 0.3 and zero. The exceedance probabilities—the probabilities that given a single kilometer of sample track, the maximum gouge depth will be equal to or greater than some indicated value, d_{max}—are shown in Figure 19. Also shown is the spatial recurrence interval for 1-km segments with one or more exceedances, which is equal to the reciprocal of the exceedance probability. This parameter gives the expected number of kilometers of sea floor that must be observed before the maximum gouge depth in one of those kilometers is expected to equal or exceed d_{max}. Another parameter of possible interest is the number of kilometers per 100 km of sample track in which the maximum gouge depth is expected to equal or exceed d_{max}. This number can be obtained simply by multiplying the appropriate exceedance probability by 100. The curves sweep across the graph and show systematic changes with water depth as was expected. The 10- to 15- and the 20- to 25-m curves, which are omitted to restrict clutter, lie as expected on the figure. The 30- to 35-m curve is very similar to the 25- to 30-m curve, which is not too surprising as there are not many d_{max} values in the 30- to 35-m range. It should also be noted that in the plots of d_{max} vs z from the Mackenzie Delta region (Lewis 1977a), the d_{max} values peak at approximately 40 m and decrease in deeper water.

In Figure 19 the 0 to 5-m data and the data from the lagoons overlap each other. As there are only three data points in the 0 to 5-m data set (as the result of censoring the lower values), the calculated curve was not particularly similar to the curves from deeper water. The curve presented in Figure 19 is based on the data from lagoons and appears to give a reasonable representation of the 0 to 5-m data points as well.

Figure 20 presents $\bar{X} = \log \bar{d}_{max}$, A, G, and S plotted as a function of $\bar{z}$. This plot should be useful to those interested in developing eq 11 to apply to other water depth intervals than those considered here. The most systematic change in a parameter with $\bar{z}$ is the roughly linear increase in $\bar{X}$.

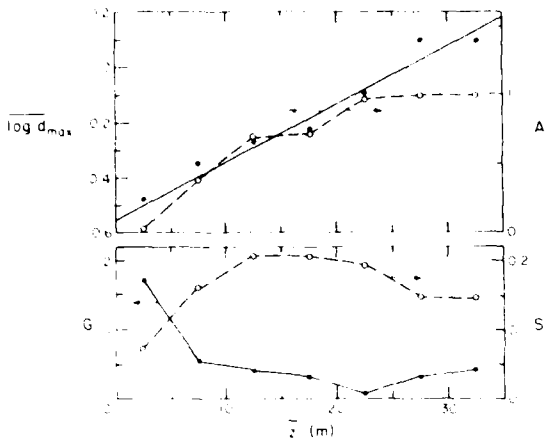

Figure 20. Parameters relating to the determination of eq 11 shown as a function of water depth ($\bar{z}$).

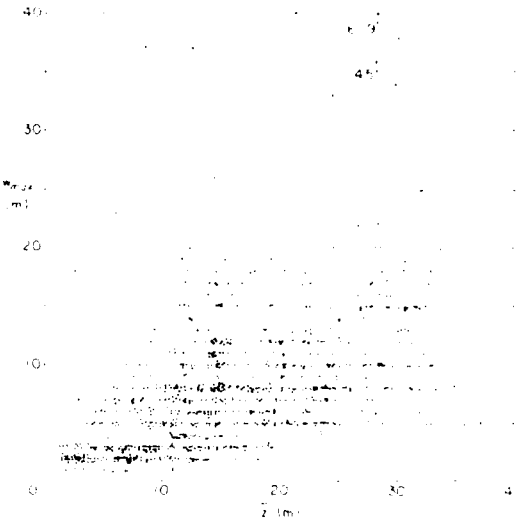

Figure 21. Plot of w_{max} for 1-km line segments vs water depth ($\bar{z}$) for all locations except lagoons.

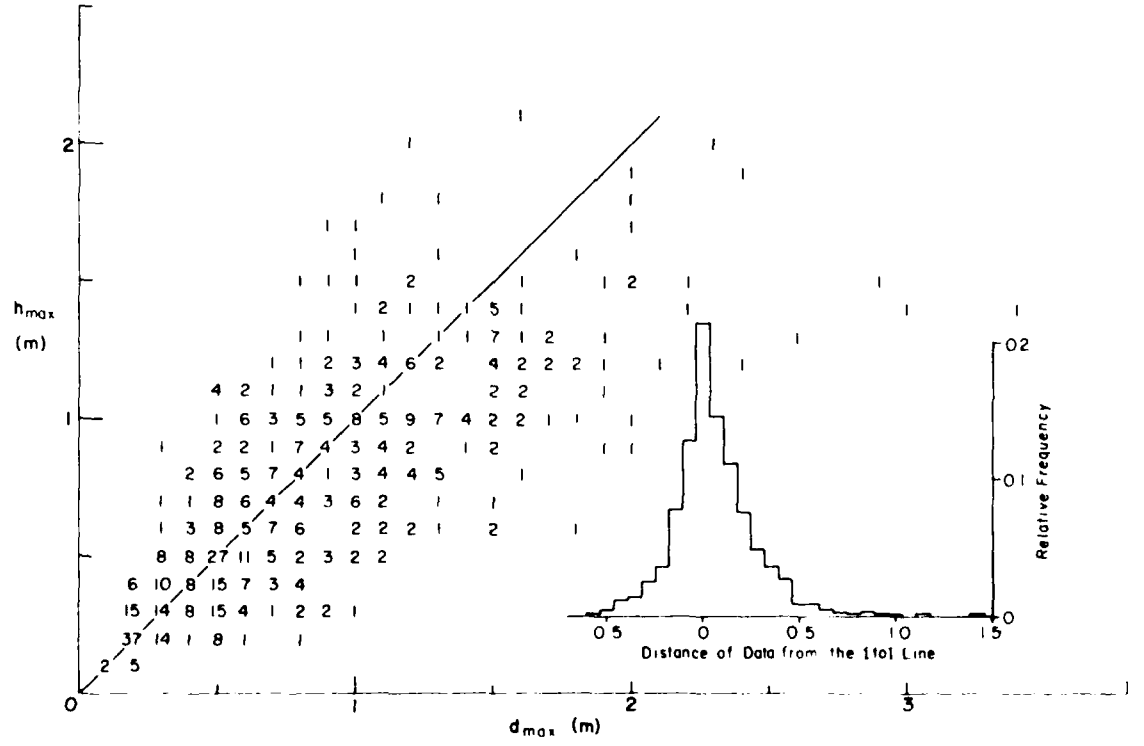

Figure 22. Plot of h_{max} vs d_{max}. Both values are for 1-km line segments. The numbers indicate the number of values present. The inset histogram shows the scatter of the data as measured normal to the 1-to-1 line.

Gouge widths

Figure 21 shows all maximum gouge widths (w_{max}) measured outside the barrier islands compared with the average water depth ($\bar{z}$). The trends are similar to those present in Figure 18, which plotted d_{max} vs average water depth. There is a general increase in w_{max} as $\bar{z}$ increases. This may simply reflect that, on the whole, gouges that are deeper are also wider. In addition, in deeper water there do not appear to be any small w_{max} values as there were in shallow water.

Lateral embankment heights

Finally, a comparison of h_{max}, the maximum lateral embankment height, and d_{max} is presented in Figure 22 (the numbers indicate the number of values). It is hardly surprising that, on the average, regions with deeper gouges should contain higher embankments as the material from the gouges produces the embankments. However, we were surprised at how symmetrically the values were distributed around the one-to-one line. This is shown by the histogram (see the inset in Fig. 22) of the relative frequency of deviations from the one-to-one line (measured normal to that line).

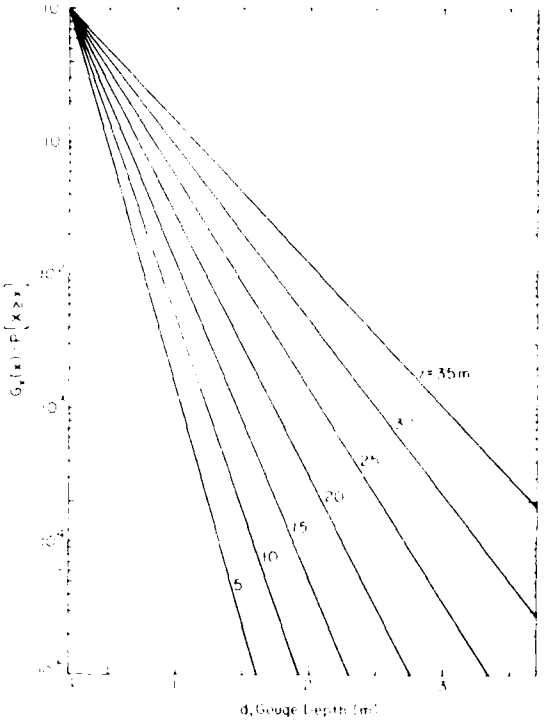

Figure 23. Plot of the exceedance probability $[G_\lambda(x)]$ vs gouge depth for different water depths (z) in the offshore region unprotected by barrier islands. In calculating the $G_\lambda(x)$ values, the λ values are obtained from the relation shown in Figure 10.

APPLICATIONS TO OFFSHORE DESIGN

In the preceeding sections we have attempted to systematize and clarify some of the essential characteristics of a large set of measurements on the geometry of ice-induced gouges in the sediments of the Alaskan portion of the shelf of the Beaufort Sea. These observations are, of course, valuable in themselves. For instance, it is useful to know that outside of the barrier islands in water up to 38 m deep the deepest gouge observed was 2.6 m, obtained from a sample of 20,313 gouges collected over 1500 km of sampling track. In the protected lagoons, on the other hand, the deepest gouge (0.7 m) was much shallower (from a sample of 41 gouges obtained from 298 km of sampling track) and a large percentage (92%) of the 1-km segments examined contained no gouges at all. In the remainder of this section we will attempt to use the data analysis performed earlier in this paper to make a series of preliminary estimates of the probability of occurrence of gouges with certain prescribed depths and frequencies.

Gouge depths

To obtain the exceedance probability for the occurrence of gouges of different depths, given that gouging has occurred, the relation in Figure 10 can be used to obtain an estimate of λ applicable to the water depth of interest. The exceedance probability is then obtained from eq 2. For instance, for a water depth of 5 m, $\hat{\lambda} = 8.16$ and

$$P[D \geq 1] = \exp[-8.16(1-0.2)] = 1.46 \times 10^{-3}$$

gives the probability of a gouge exceeding 1 m in depth. Therefore, using eq 3, one gouge in 685 would be expected to be at least 1 m deep. The 0.2-m correction in the above calculation is caused by the fact that the 0 to 0.2-m depth class was deleted in the estimation of λ. At the same water depth, one gouge in 2.39 million would be expected to be at least 2 m deep. For 35 m of water ($\hat{\lambda}$ = 2.46) things are very different; one gouge in seven exceeds 1 m and one in 980 exceeds 3 m. A graphic display of the variations in the exceedance probability as a function of water depth for the offshore region is given in Figure 23.

The $\hat{\lambda}$ values determined for lagoons appear to be in the 7- to 9-m^{-1} range, i.e. in general agreement with the $\hat{\lambda}$ values obtained from similar water depths in the offshore data set.

Extreme value statistics

It is important to note two factors concerning the extreme value statistics that have been presented. First, the sampling lines cross the gouges at a variety of angles. Therefore, from an area where the gouging is strongly aligned, the maximum value used was selected, in some cases, from a small number of gouges (when the sampling line nearly paralleled the gouges) and in other cases from a much larger number (when the sampling was perpendicular to the gouges). We have not attempted to correct the extreme value data in the manner that we corrected the observations on the observed number of gouges per kilometer (N) to the number that would be expected if the sampling were perpendicular to the gouging (N_1). We do not know how to make such a correction.

Secondly, it should be realized that the extreme value and the complete distribution techniques give estimates of two different factors. The extreme value approach provides an estimate of the number of 1-km segments that will have *at least* one gouge greater than or equal to some specified value d_{max} along a given length of sampling line. On the other hand, an estimate using the complete PDF gives the expected number of gouges along the line that are greater than or equal to d_{max}. The two estimates are not the same because a given 1-km sampling segment may have more than one gouge greater than or equal to d_{max}. Nevertheless, both approaches can be useful if applied appropriately.

Consider three 20-km pipeline routes, one in the lagoons and two at sites unprotected by islands in 5 to 10 and 25 to 30 m of water respectively. For the lagoons, the extreme value exceedance probability for 1-km sampling intervals is approximately 0.0065 and 0.00013 for gouge depths of 0.5 and 1.0 m respectively, corresponding to spatial recurrence intervals of 154 and 7692 km. Corresponding values for 5- to 10-m and 25- to 30-m water depths outside of the barrier islands are given in Table 7. Based on this table we could conclude that if one was to contemplate using an engineering technique that would encounter difficulties in the presence of gouges of 1 m or more, we would not anticipate problems in constructing a 20-km line within the lagoons. On the other hand, at water depths of 25 to 30 m we would expect to encounter gouges at least 1 m deep in roughly 15 of the 20 km.

Another parameter of interest is the probability $P(A)$ that the maximum gouge depth per kilometer will equal or exceed a given value (e.g. 1 m) along the pipeline. This is calculated as follows:

$$P(A) = 1 - P(B)$$

where $P(B)$ is the probability that the maximum gouge depth per kilometer will not equal or exceed 1 m in any of the 20 km. $P(B)$ in turn equals the probability that the maximum gouge depth per kilometer will not be ≥ 1 m in the first kilometer

Table 7. Exceedance probabilities.*

Location	*Gouge depth (m)*	*Exceedance probability*	*Spatial recurrence interval (km)*	*P(A)*
Lagoons	0.5	0.0065	154.0	0.1223
	1.0	0.00013	7692.0	2.597×10^{-3}
Outside barrier islands (depth 5 to 10 m)	0.5	0.14	7.1	0.9510
	1.0	0.011	90.0	0.1985
	2.0	0.00032	3125.0	6.381×10^{-3}
Outside barrier islands (depth 25 to 30 m)	1.0	0.76	1.3	1.0000
	2.0	0.10	10.0	0.8784
	3.0	0.012	83.0	0.2145
	4.0	0.0018	555.0	0.0354

*Given 1 km of sample track, spatial recurrence intervals for 1-km segments, and probabilities $P(A)$ that the maximum gouge depth per kilometer will equal or exceed the indicated gouge depth along a 20 km line based on the extreme value statistics

multiplied by the probability that it will not be >1 m in the second kilometer, etc. up to the twentieth kilometer. Assuming that each kilometer has the same probability $P(C)$ that the maximum gouge depth per kilometer will not be >1 m, then $P(B)$ $[P(C)]^{20}$. $P(C)$ is, however, equal to 1 minus the probability $P(D)$ that the maximum gouge depth per kilometer will be >1 m. In short,

$$P(A) = 1 - [1 - P(D)]^n \quad (12)$$

where n is the number of 1-km segments composing the line. In our example, n = 20 and $P(D)$ = 0.00013 for lagoons so that $P(A)$ = 0.0026. These values as well as similar values at water depths of 5 to 10 m and 25 to 30 m are also included in Table 7. As is shown, the probability of encountering an extreme gouge with a depth equal to or greater than 4 m in water 25 to 30 m deep is appreciably larger than the probability of encountering a 1-m extreme gouge in the lagoons.

Burial depths

The problem of burial depth can be considered in several different ways. Clearly, every gouge greater than a specified value is important, so it is necessary to use the PDF based on the complete set of gouge depths, as opposed to the extreme value distribution based on the maximum gouge in each kilometer.

First, we consider the situation where we wish to bury the pipeline at a depth so that it is all covered (assuming an acceptably low probability of encountering a gouge deeper than our burial depth that would leave the line uncovered). In this case we are dealing with gouge depths as they exist on the sea floor at a given instance of time. Again as an example we will consider a 20-km line that will be, in turn, restricted to lagoons and to water depths of 5 to 10 m and 25 to 30 m outside the barrier islands. We will also consider the case where the direction of the line is 20° off the direction of the gouges as well as normal to the direction of the gouges. For instance, at a water depth of 25 to 30 m we would expect to encounter an average of 80 gouges per kilometer if the line is normal to the gouges and 80 sin 20° = 27 gouges per kilometer if the angle between the gouges and the line is 20°. Considering 20-km lines, this corresponds to 1600 and 540 gouges, respectively. Next, one must decide how many gouges can be tolerated deeper than the depth of burial. We will take two cases: one exceedance per 20 km and one exceedance per 100 km. Burial depths (x) can then be calculated from eq 3, which, when rearranged and modified to treat the above cases, becomes

$$\frac{n[D \geq d]}{N} = \frac{n[D > d]}{N(\sin\theta)L} = e^{\lambda(x - 0.2)} \quad (13)$$

or, rearranging

$$x = 0.2 - \frac{1}{\lambda} \ln\left[\frac{n[D > d]}{N(\sin\theta)L}\right]. \quad (14)$$

As stated, at a water depth of 5 to 10 m, λ = 7.3, N = 10, θ = 20 or 90°, L = 20 or 100 km and $n[D > d]$ = 1 inasmuch as we only wish to allow one exceedance. The results of several such calculations are given in Table 8.

Unfortunately, the problem we would really like to solve is somewhat different and more difficult than the above; a pipeline is buried and we wish to estimate as a function of burial depth how often (in a time sense) the pipeline can be expected to be impacted by a pressure ridge keel. This problem also requires knowledge of the rates of occurrence

Table 8. Estimated burial depths assuming that one existing gouge will exceed the burial depth along the length of the line.

		Line normal to gouges			*Line at 20° to gouges*		
Location	λ *(m^{-1})*	N *(gouges/km)*	*Length of line (km)*	*Burial depth (m)*	$N(\sin 20)$ *(gouges/km)*	*Length of line (km)*	*Burial depth (m)*
Lagoons	7.7	0.8	20	0.56	0.27	20	0.42
			100	0.77		100	0.63
Outside barrier islands (depth 5 to 10 m)	7.3	10.0	20	0.93	3.42	20	0.78
			100	1.15		100	1.00
Outside barrier islands (depth 25 to 30 m)	3.2	80.0	20	2.51	27.36	20	2.17
			100	3.01		100	2.67

of new gouges. What length of time do the observed gouge sets represent? This question can be examined from several different viewpoints. First, we can estimate sedimentation rates in the study area to see how fast gouges would be erased (filled), assuming uniform sedimentation. Average sedimentation rates appear to be quite low. Reimnitz et al. (1977) obtained an average value of 0.06 cm yr^{-1} by dividing the observed average thickness of recent (Holocene) sediments (3 m) by the period of time their study area was believed to have been covered by the sea (5000 years). Lewis (1977a) obtained similar but generally higher values (0.05 to 0.2 cm yr^{-1}) for his study area north of the Mackenzie Delta. Using the 0.06 cm yr^{-1} value and assuming that no other processes are active, it would take about 1666 years to fill a 1-m-deep gouge and 5000 years to fill a 3-m-deep gouge. Based only on this information, an observed gouge set would represent a long period of time.

In the above, the assumption of uniform sedimentation on the shelf is probably in error. A gouged bottom morphology creates abrupt local relief and local sedimentation rate anomalies that amount to large differences in sedimentation rates over short distances. Gouge embankments may be sites of erosion while the gouges, as depressions, act as loci of much higher rates of sedimentation than would be apparent on a regional basis. Furthermore, sedimentary structures in-shore of 20 m show shelf deposits to consist of gouge infill material (Barnes and Reimnitz 1974, Barnes et al. 1979).

In addition, it is becoming increasingly apparent that shallow water gouges are rapidly obliterated due to high levels of hydrodynamic activity (Kovacs 1972, Pilkington and Marcellus 1981). For instance, recent field observations by Barnes and Reimnitz (1979) show that the extensive open-water conditions that occurred during the summer of 1977 resulted in hydrodynamic conditions (presumably, large waves and wind-generated shelf currents associated with the presence of a large fetch) that have obliterated ice gouges to a water depth of 13 m and caused pronounced infilling of gouges in deeper water. Apparently, the rates of reworking and redepositing sediment from such episodic events are much greater than the average sediment accumulation rate on the Beaufort Sea shelf.

We know of no studies of the recurrence frequency of conditions such as those observed during the summer of 1977, but we would guess that they are fairly common, with return periods of no more than 25 years. Twenty-five years appears to be a reasonable estimate for the return period of significant storm surges along the coast of the Beaufort Sea (Reimnitz and Maurer 1978), events that would presumably be associated with similar or more energetic hydrodynamic conditions. In short, although sedimentation rates might lead one to believe that the Beaufort Shelf is a rather static environment sedimentologically, this is far from the case; particularly in locations where water depths are less than 10 m.

Therefore, in most of the area we have studied, we would not have confidence in the assumption that the sea floor, as seen at a given time, represents a steady-state condition with the number of new gouges per unit time equaling the number of gouges infilled by sedimentation plus the number of new gouges superimposed on existing gouges. Such statistical time invariance of the gouging is an essential assumption if the rate of production of new gouges is estimated using the scour budget approach developed by Lewis (1977a,b). We think the method is interesting and quite possibly applicable to certain regions of gouging, for instance offshore areas in the Chukchi Sea with water depths of 30 to 50 m. However, for the Beaufort Sea in general, and in particular for water depths less than 20 m, we feel that the applicability of the steady-state assumption is doubtful.

Another approach used to get a rough estimate of the age of an observed set of gouges is to divide the average value for the annual sum of the gouge widths by the length of the sample track (Reimnitz et al. 1977a). For instance, if our sample line is 10 km long and we obtain an average of 500 m of new gouges crossing the line each year, we then take 20 years as an estimate of the time period in which the gouges are completely replaced. In fact, such estimates give the shortest period of time in which the gouge set could be replaced (an event of very low probability), as ice presumably plows the sea floor in a random (not a systematic) manner. Therefore, the fact that a given segment of a line has just been gouged has no effect on the probability that the segment will be gouged the next year (or the next month).

Still another approach using the same data set assumes that an increasingly large proportion of the bottom is regouged before the entire bottom is gouged (Barnes et al. 1978). In this scheme, if 10% of the seabed is gouged each year then in the first year 10% is impacted with new gouges but in the second year only 19% is gouged as 1% of the

gouges occurred in areas already gouged. This can be expressed as the polynomial

$$G_t = 1 - (1 - K)^T \quad (15)$$

where G_t is the fraction of the bottom gouged since T_0, K is the fraction of the bottom gouged each year, and T is the time in years measured relative to T_0.

Finally, attempts have been made to combine information on pressure ridge keels, pack ice drift, and observed distributions of gouge depths to estimate required burial depths (Pilkington and Marcellus 1981, Wadhams 1983). As the first two of these parameters are very poorly known, such estimates are uncertain. This technique also appears to give maximum gouge depths that are appreciably deeper than observed. More will be said about this later.

We believe that at present to examine adequately the problem of pipeline burial, independent information on gouging rates and the depths of recent gouges is essential. As we have described, our information on this subject is hardly what we would desire. Nevertheless it is enough to allow us to make an initial approach to estimating burial depths. To summarize our observations on recent gouges, we found that $\bar{g}$, the number of gouges per km per year, varied from 2.4 to 7.9 with a mean of 5.2. There also was no apparent relation between $\bar{g}$ and water depth. The PDF for recent gouges was exponential with a $\hat{\lambda}$ value of 4.5 m^{-1}, a value that is 1 m^{-1} less than comparable $\hat{\lambda}$ values from all the gouges existing on the sea floor at a given time.

Using this information we can now make preliminary estimates of the burial depths required so that a pipeline of a given length will, on the average, be gouged once during a specified period of time (for instance, one time in 100 or in 1000 years). To do this, first estimate N, the total number of gouges that will occur during the proposed lifetime of the pipeline by

$$N = \bar{g} T l \sin\theta \quad (16)$$

where $\bar{g}$ = average number of gouges km^{-1} yr^{-1} occurring along the pipeline route
T = proposed lifetime in years
l = length of the line in kilometers
θ = angle betwen the route and the trend of the gouges.

As we only consider one contact in T, $N[D > d]$ in eq 3 equals 1 and we obtain

$$e^{-\lambda(x - 0.2)} = \frac{1}{\bar{g} T l \sin\theta} \quad (17)$$

or

$$x = 0.2 + \frac{1}{\lambda} \ln\left[\frac{1}{\bar{g} T l \sin\theta}\right] . \quad (18)$$

In Table 9 we show a series of burial depth estimates made using eq 18. In these calculations we have used both the observed $\hat{\lambda}$ value for the existing gouge set from Figure 10 as well as $\hat{\lambda} - 1$ as an estimate of the corresponding parameter for new

Table 9. Estimated burial depths assuming one contact between a pressure ridge keel and the pipeline in 100 years. (Calculations made using eq 18.)

				Line normal to gouges		*Line at 20° to gouges*	
Location	$\bar{g}$ *(gouges km^{-1} yr^{-1})*	λ *(or $\lambda - 1$) (m^{-1})*	*Length of line (km)*	*Gouges crossing line during 100-yr lifetime*	*Burial depth (m)*	*Gouges crossing line during 100-yr lifetime*	*Burial depth (m)*
Lagoons	5	7.7	20	10,000	1.40	3,420	1.26
		7.7	100	50,000	1.61	17,101	1.61
		6.7	20	10,000	1.57	3,420	1.41
		6.7	100	50,000	1.81	17,101	1.81
Outside barrier islands (depth 5 to 10 m)	5	7.3	20	10,000	1.46	3,420	1.31
		7.3	100	50,000	1.68	17,101	1.54
		6.3	20	10,000	1.66	3,420	1.49
		6.3	100	50,000	1.92	17,101	1.75
Outside barrier islands (depth 25 to 30 m)	5	3.2	20	10,000	3.08	3,420	2.74
		3.2	100	50,000	3.58	17,101	3.25
		2.2	20	10,000	4.39	3,420	3.90
		2.2	100	50,000	5.12	17,101	4.63

Table 10. Comparisons between burial depths to the top of a 76-km pipeline for a 1000-, 100-, and 10-year return period.*

Lifetime (yrs)	*Water depth (m)*	λ	*Scour (m)*	*Burial depth (m)*	*Source*
1000	15	5	5.5	2.54	This paper (eq 18)
		5	4.5	3.06	
		10	5.5	2.66	
		10	4.5	3.21	
	15			6.24	Wadhams (1983)
	25	5	3.7	3.67	This paper
		5	2.7	4.96	
		10	3.7	3.86	
		10	2.7	5.22	
	25			8.10	Wadhams (1983)
100	15	5	5.5	2.12	This paper
		5	4.5	2.54	
		10	5.5	2.24	
		10	4.5	2.70	
	15			4.40	Pilkington and Marcellus (1981)
	15			5.50	Wadhams (1983)
	25	5	3.7	3.05	This paper
		5	2.7	4.11	
		10	3.7	3.24	
		10	2.7	4.36	
	25			4.70	Pilkington and Marcellus (1981)
	25			7.02	Wadhams (1983)
10	15	5	5.5	1.70	This paper
		5	4.5	2.03	
		10	5.5	1.82	
		10	4.5	2.19	
	15			4.76	Wadhams (1983)
	25	5	3.7	2.43	This paper
		5	2.7	3.25	
		10	3.7	2.62	
		10	2.7	3.51	
	25			5.94	Wadhams (1983)

*Calculated using eq 18 and by Pilkington and Marcellus (1981) and Wadhams (1983).

gouges. In using the table, note that a 20-year lifetime for a 100-km line is identical to a 100-year lifetime for a 20-km line. As can be seen in the table, it is very important to obtain data that will allow improved estimates of λ and $\bar{g}$ for new gouges. In general it can be said that slight increases in the burial depth (a few tens of centimeters) result in appreciable increases in the safety of the line. This statement is particularly true in shallow water where λ is large.

In Table 10 we have also included a comparison between our estimates of burial depths and those of Pilkington and Marcellus (1981) and of Wadhams (1983) for a 76-km line (the distance from the artificial gravel island Kopanoar to the shore). The return period for an impact is taken to be 10, 100, and 1000 years. There are large differences in the estimates, with our burial depths being roughly 3 m less than Wadhams. In fact, for the 25-m water depth our estimates would only be 4.05 and 5.47 m (assuming λ = 3.7 and 2.7 respectively) if we took g to be 20; a value 4 times that observed. We believe the difficulty with Wadhams' approach lies not in its principles but in the difficulty of obtaining appropriate values to use in the theory. For instance, keel depth characteristics in deeper water where it is possible to probe the underside of the ice via submarine are probably appreciably different from those in water of 50 m or less where gouging is currently taking place. In

addition, it is at present particularly difficult to know what values to assume for the distance drifted per year by the ice cover over a given point. When gouging starts, the ice is slowed and many times stopped, as the grounded ice tends to stabilize the nearby pack, converting it to fast ice.

The differences between our estimates and those of Pilkington and Marcellus (1981) are less by 1 to 2 m than our differences with Wadhams' estimates; we find this somewhat surprising as their procedures appear to be essentially identical. The differences in their estimates would appear to be largely the result of differences in the data used to estimate the number of gouges km^{-1} yr^{-1}. In that Wadhams used direct observations of keels while Pilkington and Marcellus indirectly inferred the number of keels from laser measurements of ridge sails, one would expect Wadhams' number to be more realistic. Clearly we are a long way from achieving a consensus regarding suitable pipeline burial depths.

CONCLUSION

In this paper we have presented a large amount of data on the statistical characteristics of the ice-produced gouges that occur on the Alaskan shelf of the Beaufort Sea in shallow water (< 38 m). Although at first glance the gouges appear to be rather chaotically distributed, in a statistical sense they are very systematic. Consequently we have used this information to estimate the requisite burial depths of pipelines that would allow one hit by an ice mass in a specified number of years.

In conclusion we would like to comment on some problems, the study of which would contribute to the understanding of the geophysics of gouging and to the safe design of sea-floor pipelines in regions where gouging is known to occur. We believe the weakest link in the present study is the paucity of information on the rate of occurrence of new gouges and their characteristics. Field programs should be expanded to collect this type of information. In areas where offshore development is contemplated, it is important to start studies of gouging rates as soon as possible, as the collection of an adequate data set takes several years.

Systematic regional sampling is also required to reveal changes, if any, in the probability density functions of parameters such as gouge depth with changes in location and in environment on the shelf. Current information suggests that there are appreciable changes in such parameters on a regional scale (for instance, between the gouge depths in the present study area and those observed off the Mackenzie Delta). Studies should also be carried out to quantify the effects on gouging of differences in slope angle and aspect and the nature of bed material. Such work, in conjunction with detailed site-specific studies, would be very useful in evaluating hazards along specific pipeline routes.

Theoretical studies should also be implemented to advance our ability to treat gouging as a stochastic process. For instance, it would be useful to look at gouging as a simple covering problem in geometric probability. If such developments are sufficiently general, they can be applied to different geographic areas by simply changing the values of the input parameters.

We also note that although we have utilized an exponential distribution to describe the relative frequency of occurrence of gouges of different depths because of its simplicity and the fact that pressure ridge keels can be well described by such a distribution, χ^2 tests of goodness of fit are commonly failed. Therefore attempts should be made to obtain a more satisfactory distribution to describe gouge depths. The same general comment can be made about our utilization of a Poisson distribution to describe N in that, as was noted earlier, there are consistently more large N (10) values than predicted by the fitted Poisson. We suggest that at least some of these difficulties arise from the fact that there is no adequate treatment of the infilling of the gouges in either this or other published papers on gouging. The development of a numerical simulation model that includes a description of both initial gouging and subsequent infilling of existing gouges could prove to be illuminating.

Finally, it would be useful to improve our understanding of the interactions between pressure ridge and ice island keels and the sea floor. Perhaps such studies will provide insight into the possibility of determining maximum probable gouge depths for a given sediment type. Until such information is available, we can only assume that even apparently "impossibly" deep gouges have a finite probability of occurrence.

LITERATURE CITED

Alaska Projects Office (APO) (1978) Environmental assessment of the continental shelf, interim

synthesis: Beaufort Chukchi. Study by U.S. Army Cold Regions Research and Engineering Laboratory (CRREL) Alaska Projects Office (APO) for National Oceanic Atmospheric Administration, Outer Continental Shelf Environmental Assessment Program, Environment Research Laboratories, Boulder, Colorado.

Barnes, P.W. and D. McDowell (1978) New bathymetric Outer Continental Shelf map of the Alaskan Beaufort Sea. NOAA, Outer Continental Shelf Environmental Assessment Program, Quarterly Reports of Principal Investigators, April June 1978, pp. 267-269 and Figure 1.

Barnes, P.W. and E. Reimnitz (1974) Sedimentary processes on Arctic shelves off the north coast of Alaska. In *The Coast and Shelf of the Beaufort Sea* (J.C. Reed and J.E. Sater, Eds.). Arlington, Virginia: Arctic Institute of North America, pp. 439-476.

Barnes, P.W. and E. Reimnitz (1979) Ice gouge obliteration and sediment redistribution event, 1977-1978, Beaufort Sea, Alaska. U.S. Geological Survey Open File Report 79-848, 22 pp.

Barnes, P.W., D. McDowell and E. Reimnitz (1978) Ice gouging characteristics: Their changing patterns from 1975-1977, Beaufort Sea, Alaska. U.S. Geological Survey Open File Report 78-730, 42 pp.

Barnes, P.W., E. Reimnitz, L.J. Toimil, P.K. Maurer and D. McDowell (1979) Core descriptions and preliminary observations of vibracores from the Alaskan Beaufort Sea shelf. U.S. Geological Survey Open File Report 79-351, 106 pp.

Benjamin, J.R. and C.A. Cornell (1970) *Probability, Statistics and Decision for Civil Engineers.* New York: McGraw-Hill, 684 pp.

Fredsoe, J. (1979) Natural backfilling of pipeline trenches. *Journal of Petroleum Technology*, October, pp. 1223-1230.

Haan, C.T. (1977) *Statistical Methods in Hydrology.* Ames, Iowa: Iowa State University Press, 378 pp.

Hahn, G.J. and S.S. Shapiro (1967) *Statistical Models in Engineering.* New York: Wiley and Sons, 355 pp.

Hnatiuk, J. and K.D. Brown (1977) Sea bottom scouring in the Canadian Beaufort Sea. Ninth Annual Offshore Technology Conference, Houston, Texas, Paper OTC 2946, pp. 519-527.

Hopkins, D.M. (1967) The cenozoic history of Beringia—A synthesis. In *The Bering Land Bridge* (D.M. Hopkins, Ed.). Stanford, California: Stanford University Press, pp. 451-484.

Kindle, E.M. (1924) Observations on ice-bourne sediments by the Canadian and other arctic expeditions. *American Journal of Science*, **7**: 251-286.

Kovacs, A. (1972) Ice scoring marks floor of the Arctic shelf. *The Oil and Gas Journal*, **70**: 92-106.

Kovacs, A. (1976) Grounded ice in the fast ice zone along the Beaufort Sea coast of Alaska. USA Cold Regions Research and Engineering Laboratory, CRREL Report 76-32, 21 pp. ADA 031352.

Kovacs, A. (1979) Recent ice observations in the Alaskan Beaufort Sea Federal-State lease area. *The Northern Engineer*, **10**: 7-12.

Kovacs, A. and M. Mellor (1974) Sea ice morphology and ice as a geologic agent in the southern Beaufort Sea. In *The Coast and Shelf of the Beaufort Sea* (J.C. Reed and J.E. Sater, Eds.). Arlington, Virginia: Arctic Institute of North America, pp. 113-161.

Kovacs, A. and D.S. Sodhi (1980) Shore ice pile-up and ride-up: Field observations, models, theoretical analyses. *Cold Regions Science and Technology*, **2**: 209-288.

Lewis, C.F.M. (1977a) Bottom scour by sea ice in the southern Beaufort Sea. Department of Fisheries and the Environment, Beaufort Sea Technical Report 23 (draft). Beaufort Sea Project, Victoria, British Columbia, 88 pp.

Lewis, C.F.M. (1977b) The frequency and magnitude of drift ice groundings from ice-scour tracks in the Canadian Beaufort Sea. In *Proceedings, 4th International Conference on Port and Ocean Engineering Under Arctic Conditions.* Memorial University, Newfoundland, **1**: 567-576.

Mardia, K.V. (1972) *Statistics of Directional Data.* New York: Academic Press, 357 pp.

Mathews, J.B. (1981) Observations of surface and bottom currents in the Beaufort Sea near Prudhoe Bay, Alaska. *Journal of Geophysical Research*, **86**(C7): 6653-6660.

Miller, I. and J.E. Freund (1977) *Probability and Statistics for Engineers.* New York: Prentice-Hall, 529 pp.

Pelletier, B.R. and J.M. Shearer (1972) Sea bottom scouring in the Beaufort Sea of the Arctic Ocean. 24th International Geological Congress, Section 8, Marine Geology and Geophysics, Montreal, pp. 251-261.

Pilkington, G.R. and R.W. Marcellus (1981) Methods of determining pipeline trench depths in the Canadian Beaufort Sea. In *POAC '84 Proceedings, The 6th International Conference*, **II**: 674-687.

Rearic, D.M., P.W. Barnes and E. Reimnitz (1981) Ice-gouge data, Beaufort Sea, Alaska, 1972-1980. U.S. Geological Survey Open File Report 81-950, 23 pp.

Reimnitz, E. and P.W. Barnes (1974) Sea ice as a geologic agent on the Beaufort Sea shelf of Alaska. In *The Coast and Shelf of the Beaufort Sea* (J.C. Reed and J.E. Sater, Eds.). Arlington, Virginia: Arctic Institute of North America, pp. 301-353.

Reimnitz, E. and D.K. Maurer (1978) Storm surges in the Alaskan Beaufort Sea. U.S. Geological Survey Open File Report 78-593, 26 pp.

Reimnitz, E., P.W. Barnes, T.C. Forgatsch and C.H. Rodeick (1972) Influence of grounding ice on the Arctic shelf of Alaska. *Marine Geology*, **13**: 323-334.

Reimnitz, E., P.W. Barnes and T.R. Alpha (1973) Bottom features and processes related to drifting ice on the Arctic Shelf, Alaska. U.S. Geological Survey, Miscellaneous Field Studies Map MF-532.

Reimnitz, E., P.W. Barnes, L.J. Toimil and J. Melchior (1977a) Ice gouge recurrence and rates of sediment reworking, Beaufort Sea, Alaska. *Geology*, **5**: 405-408.

Reimnitz, E., L.J. Toimil and P.W. Barnes (1977b) Stamukhi zone processes: Implications for developing the Arctic offshore. Ninth Annual Offshore Technology Conference, Houston, Texas, Paper OTC 2945, pp. 513-518.

Reimnitz, E., L.J. Toimil and P.W. Barnes (1978) Arctic continental shelf morphology related to sea-ice zonation, Beaufort Sea, Alaska. *Marine Geology*, **28**: 179-210.

Shearer, J.M. and S.M. Blasco (1975) Further observations of the scouring phenomena in the Beaufort Sea. In *Report of Activities, Part A*. Geological Survey of Canada, Paper 75-1A, pp. 483-493.

Shearer, J.M., E.F. MacNab, B.R. Pelletier and T.B. Smith (1971) Submarine pingos in the Beaufort Sea. *Science*, **174**: 816-818.

Skinner, B.C. (1971) Investigation of ice island scouring of the northern continental shelf of Alaska. U.S. Coast Guard Academy Report RDC GA-23, 24 pp.

Slack, J.R., J.R. Wallis and N.C. Matalas (1975) On the value of information to flood frequency analysis. *Water Resources Research*, **11**: 629-647.

Thomas, D.R. and R.S. Pritchard (1979) Beaufort and Chukchi Sea ice motions. Part I: Pack ice trajectories. FLOW Research Report No. 133. Kent, Washington: FLOW Research Company.

Tucker, W.B., W.F. Weeks and M.D. Frank (1979) Sea ice ridging over the Alaskan continental shelf. *Journal of Geophysical Research*, **84**(C8): 4885-4897.

U.S. Water Resources Council (USWRC) (1977) *Guidelines for Determining Flood Flow Frequency*. Bulletin 17A of the Hydrology Committee. Washington, D.C.: United States Water Resources Council, 163 pp.

Wadhams, P. (1983) The prediction of extreme keel depths from sea ice profiles. *Cold Regions Science and Technology*, **6**(3): 257-266.

Wadhams, P. and R.J. Horne (1980) An analysis of ice profiles obtained by submarine sonar in the Beaufort Sea. *Journal of Glaciology*, **25**(93): 401-424.

Wahlgren, R.V. (1979a) Ice-scour tracks on the Beaufort Sea continental shelf—Their form and an interpretation of the processes creating them. M.A. Thesis, Department of Geography, Carleton University, Ottawa, 183 pp.

Wahlgren, R.V. (1979b) Ice-scour tracks in eastern Mackenzie Bay and north of Pullen Island, Beaufort Sea. In *Current Research, Part B*. Geological Survey of Canada, Paper 79-1B, pp. 51-62.

APPENDIX A: DETAILED BATHYMETRIC MAP OF THE ALASKAN PORTION OF THE BEAUFORT SEA

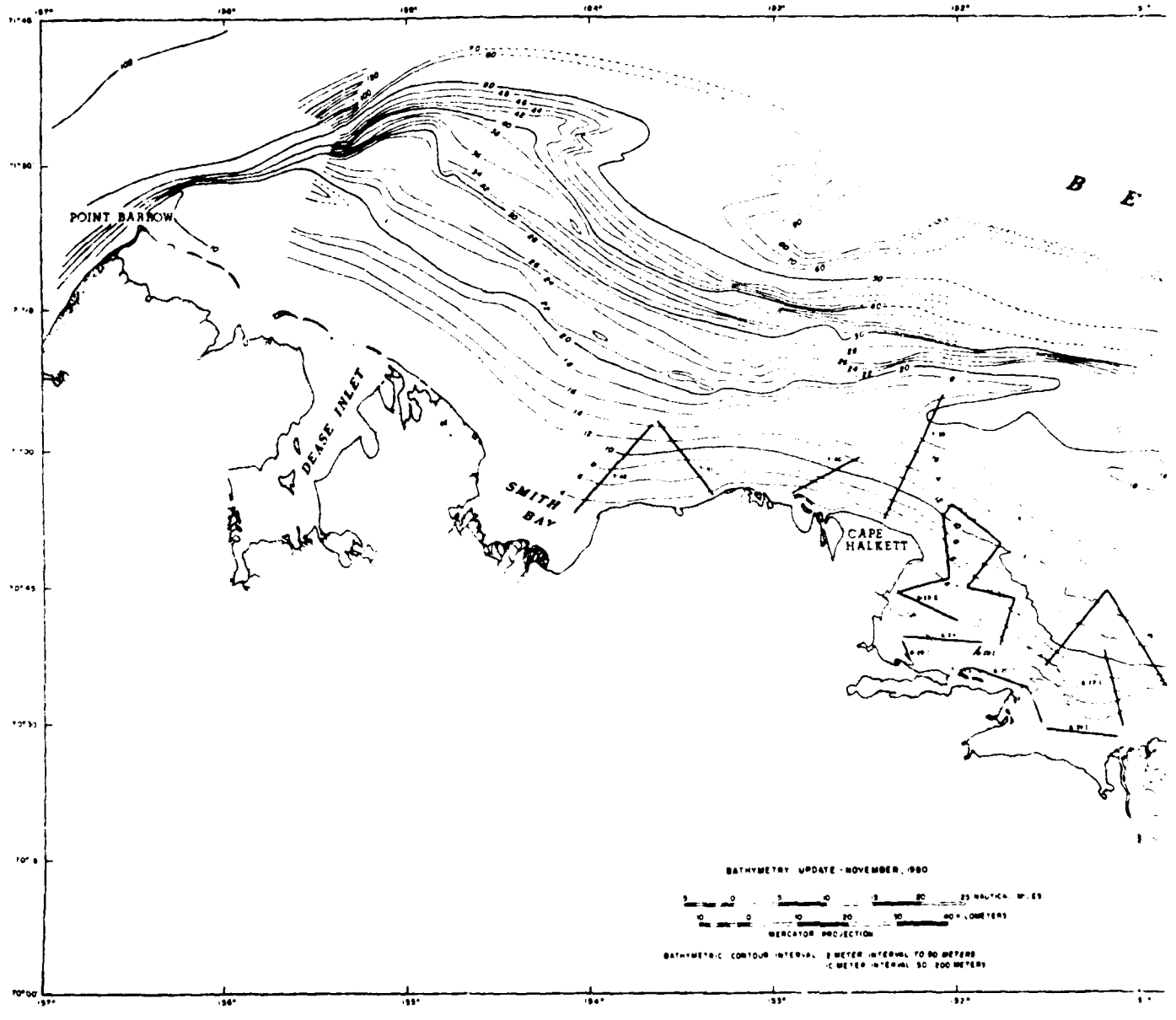

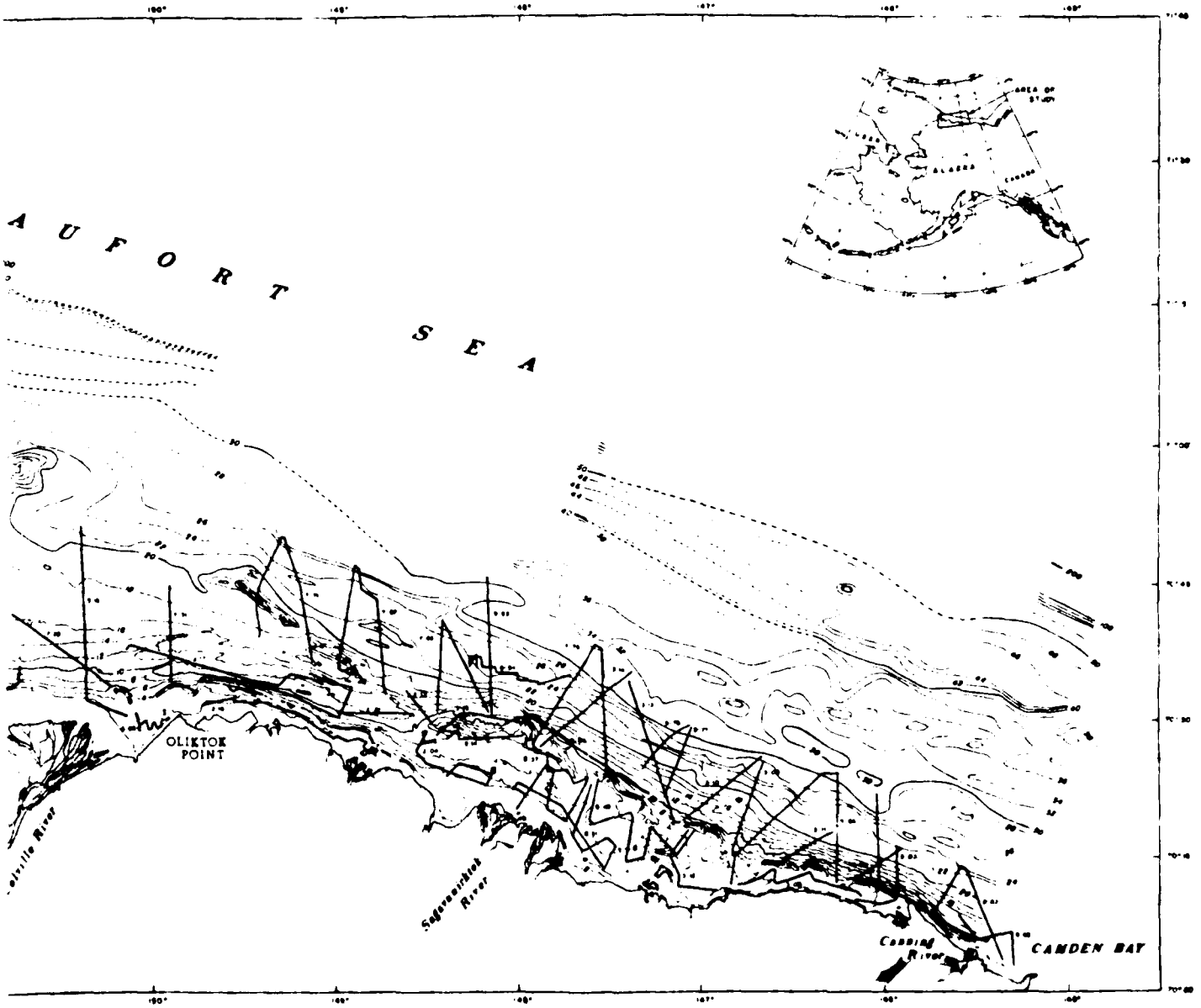
A U F O R T S E A
OLIKTOK POINT
Sagavanirktok River
CAMDEN BAY

A facsimile catalog card in Library of Congress MARC format is reproduced below.

Weeks, W.F.
Statistical aspects of ice gouging on the Alaskan Shelf of the Beaufort Sea / by W.F. Weeks, P.W. Barnes, D.M. Rearic and E. Reimnitz. Hanover, N.H.: U.S. Cold Regions Research and Engineering Laboratory; Springfield, Va.: available from National Technical Information Service, 1983.
v, 40 p., illus., 28 cm. (CRREL Report 83-21)
Bibliography: p. 32.
1. Arctic Ocean. 2. Arctic regions. 3. Beaufort Sea. 4. Ice. 5. Ice gouging. 6. Sea ice. 7. Offshore drilling. 8. Offshore structures. I. Barnes, P.W. II. Rearic, D.M. III. Reimnitz, E. IV. United States. Army. Corps of Engineers. V. Cold Regions Research and Engineering Laboratory, Hanover, N.H. VI. Series: CRREL Report 83-21.

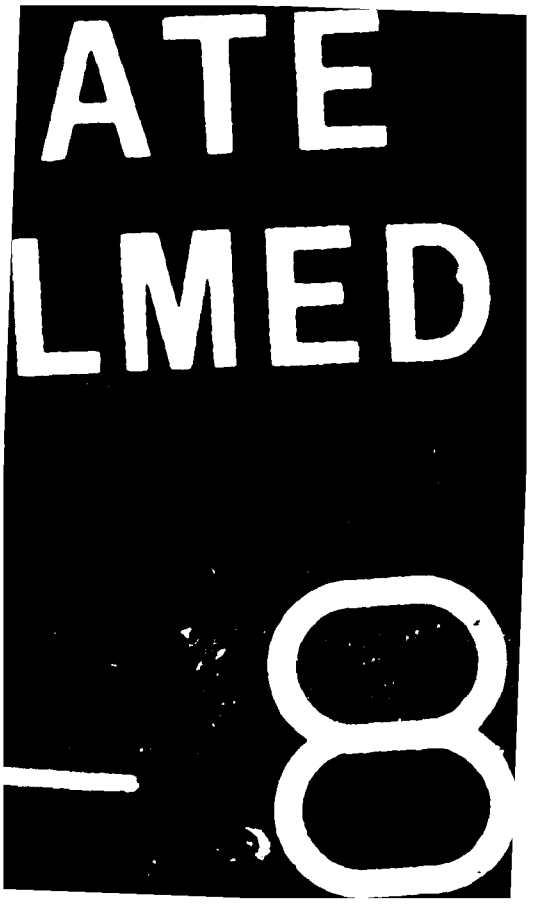
ATE
LMED
8